Aquaculture 568 (2023) 739318

Contents lists available at ScienceDirect

Aquaculture

journal homepage: www.elsevier.com/locate/aquaculture

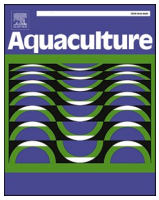

From invasion to fish fodder: Inclusion of the brown algae *Rugulopteryx okamurae* in aquafeeds for European sea bass *Dicentrarchus labrax* (L., 1758)

Filomena Fonseca [a,f,*], Juan Fuentes [b], Antonio Jesús Vizcaíno [c], Francisco Javier Alarcón [c], Juan Miguel Mancera [d], Gonzalo Martínez-Rodríguez [e], Juan Antonio Martos-Sitcha [d,**]

[a] Centro de Investigação Marinha e Ambiental (CIMA), Universidade do Algarve, 8000-139 Faro, Portugal
[b] Centre of Marine Sciences (CCMar), Universidade do Algarve, Faro, Portugal
[c] Department of Biology and Geology, Campus de Excelencia Internacional del Mar (CEI·MAR), University of Almería, 04120 Almería, Spain
[d] Department of Biology, Faculty of Marine and Environmental Sciences, Instituto Universitario de Investigación Marina (INMAR), Campus de Excelencia Internacional del Mar (CEI·MAR), University of Cádiz, 11519 Puerto Real, Cádiz, Spain
[e] Institute of Marine Sciences of Andalusia, Spanish National Research Council (ICMAN-CSIC), 11519 Puerto Real, Cádiz, Spain
[f] ARNET - Aquatic Research Network - Associate Laboratory, Universidade do Algarve, 8000-139 Faro, Portugal

ARTICLE INFO

Keywords:
Algae-based aquafeeds
Fish gut microbiota
Fish immune-related genes
Fish intestine electrophysiology
Fish intestinal epithelium

ABSTRACT

In keeping with the premises of Blue Circular Economy in the European Union, the present study explored the possibility of using the invasive brown alga *Rugulopteryx okamurae* in aquafeeds for European sea bass *(Dicentrarchus labrax)*. Assuming the raw algae biomass could negatively impact animal performance, four experimental formulations were prepared, by including macroalgae material at 5%, using crude (CR), enzymatically hydrolysed and fermented (EF), enzymatically hydrolysed (E), or fermented (F) *R. okamurae* biomass, which we tested against a control feed (CT). To evaluate the effects of the experimental diets, besides animal growth performance and biometric parameters, we devised a toolbox focused on the intestine and intestinal function: i) ex-vivo epithelial resistance and permeability in Ussing chambers; ii) microbiota composition through NGS; iii) expression profiles of selected markers for epithelial integrity, transport, metabolism, and immune response, by qPCR. Our results show differentiated allometric growth among diets, coupled with intestinal epithelium alterations in permeability, integrity, and amino acid transport. Additionally, evidence of microbiota dysbiosis and contrasting immune responses between experimental diets, i.e. pro-inflammatory vs. anti-inflammatory, are also described. In conclusion, we believe that *R. okamurae* could be a suitable resource for aquafeeds for the European sea bass, although its use requires a pre-treatment before inclusion. Otherwise, while the fish still have a positive growth performance, the gastrointestinal tract pays a toll on the integrity, transport, and inflammatory processes.

1. Introduction

The exotic brown algae *Rugulopteryx okamurae* has expanded with large amounts of biomass in southern Europe, bearing one of the most important causes of biodiversity loss by profoundly affecting the structure and functioning of native communities (Steen et al., 2017). Thus, the rapid expansion of *R. okamurae* has caused a significant impact on the pre-established benthic communities, as well as the accumulation of thousands of tons of algae from its arrival and severe problems of snagging in fishing nets (García-Gómez et al., 2020). Therefore, it is crucial to coordinate plans for removal or elimination by sustainable use and to exploit the large amounts of algal biomass available.

Marine seaweeds, such as brown algae (*Phaeophyceae*), are characterized not only by having a protein content that ranges between 3 and 15% and lipid content of 0.4–5% dry weight but also by containing bioactive compounds of potential interest, such as polysaccharides, pigments (chlorophyll and carotenoids), sterols, terpenoids, polyphenols, and vitamins (Silva et al., 2015; Moutinho et al., 2018). The *Dictyotaceae* family, to which *R. okamurae* belongs, has been studied specifically for their high content of secondary metabolites, especially from the terpene group (Paula et al., 2011), as bioactive molecules with antimicrobial, anti-inflammatory, antifungal and antitumoral activity.

* Corresponding author at: Centro de Investigação Marinha e Ambiental (CIMA), Universidade do Algarve, Faro, Portugal.
** Corresponding author.
E-mail addresses: ffonseca@ualg.pt (F. Fonseca), juanantonio.sitcha@uca.es (J.A. Martos-Sitcha).

https://doi.org/10.1016/j.aquaculture.2023.739318
Received 9 September 2022; Received in revised form 30 January 2023; Accepted 31 January 2023
Available online 4 February 2023

Therefore, their inclusion at low levels in aquafeed formulations could benefit farmed fish, giving them a significant nutraceutical character under farming conditions. Indeed, previous studies have evaluated the potential of several macroalgae as a source of protein and functional ingredients in aquafeeds (Zhu et al., 2016; Peixoto et al., 2019), including immunostimulatory effects and improvements on the oxidative metabolism of gilthead sea bream (*Sparus aurata*) juveniles when fed on a diet including rancid oil (Martínez-Antequera et al., 2021).

The sustainable use of invasive algae as an aquafeed ingredient would comply with several principles of the European Union Blue Circular Economy. However, the inclusion of *R. okamurae* in aquafeeds, even at low levels, has two main obstacles. On the one hand, this species contains vacuoles of sulfuric acid. On the other hand, it possesses high concentrations of chemical compounds such as dilkamural, recently described to have anti-herbivory properties and contribute to the species' invasion success (Casal-Porras et al., 2021). In addition, *R. okamurae* has a high fibre content (cellulose, alginates, fucans and laminarans) in the cell wall that would act as a physical barrier, hindering the release of potentially bioactive compounds and other nutrients and maybe anti-nutritional compounds, contained in the algal biomass (Siriwardhana et al., 2004).

These properties of *R. okamurae* could be a disadvantage for carnivorous fish species, as they can also affect feed intake, growth performance and fish health. Therefore, processing prior inclusion of the algae biomass could be an essential procedure to break the cell walls, thus improving nutrient bioavailability (Tibbetts, 2018). Previous studies show promising results in enhancing accessibility to intracellular nutrients when macroalgae such as *Gracilaria gracilis* and *Ulva rigida* underwent physical-mechanical and enzymatic pre-treatments. These treatments yielded changes in the protein profile of the algae, lessening the presence of high molecular weight proteins, and increasing those of low molecular weight, such as small peptides and free amino acids (Valente et al., 2006; Batista et al., 2020).

Among the treatments used for algal cell wall rupture, enzymatic and fermentative pre-treatments have gained importance, showing more effective and profitable results on several physiological aspects, such as health and growth in farmed fish (Demuez et al., 2015; Molina-Roque et al., 2022). The inclusion of algae in low percentages in the diet of other commercial species, such as the sea bream (*S. aurata*), pre-treated by physical-mechanical processes, revealed an improvement in the innate immune response of the mucus (Reis et al., 2021). Additionally, in the red tilapia (*Oreochromis* sp.), supplementation with 15% *Ulva* sp. biomass promoted growth performance and feed conversion ratios (El-Tawil, 2010). According to other studies, the inclusion of various species of macroalgae as dietary supplement in European sea bass (*Dicentrarchus labrax*) was without effects on growth but improved the innate immune response at low percentages of inclusion (Valente et al., 2006; Peixoto et al., 2016, 2019). These observations point to clear species-specific effects depending on the algae included in aquafeeds and the target fish species.

Our premise in this work with *Rugulopteryx okamurae* and European sea bass (*Dicentrarchus labrax*) was that including the raw algae in the diet would negatively impact performance. Therefore, the algal biomass was subjected to different pre-treatments, including enzymatic hydrolysis and/or fermentation processes, to re-purpose a seemingly harmful ingredient. We targeted the whole-body effect, especially markers of performance. In addition, we focused on the intestinal level, as the gastrointestinal tract receives or suffers the first impact of feeds and devised a toolbox to understand the effects of *R. okamurae* inclusion on gut microbiota, epithelial function and molecular intestinal markers related to integrity, amino acid transport, metabolic enzymes, and immune response.

2. Materials and methods

2.1. Ethics

Fish were kept and handled following the guidelines for experimental procedures in animal research of the Ethics and Animal Welfare Committee of the University of Cadiz, according to the Spanish (RD53/2013) and European Union (2010/63/EU) legislation. The Ethical Committee from the Autonomous Andalusian Government approved the experiments (Junta de Andalucía reference number 04/04/2019/056).

2.2. Algae collection and processing

Rugulopteryx okamurae biomass (30 kg) was collected at 3 m depth from La Caleta de Tarifa beach (Cádiz, Spain). The seaweed was washed well in tap water to remove the foreign particles and then dried in a forced-air chamber (Airfrío, Almería) at 30 °C for 12 h. As structural polysaccharides are not well digested by fish and compromise the nutritional value of algae, two biological treatments (microbial fermentation and enzymatic hydrolysis) were applied for increasing the nutritional value and nutrient bioavailability. Both procedures are common techniques applied to algae for using in aquafeeds (Fernandes et al., 2022; Sáez et al., 2022; Felix and Brindo, 2014). The dried algae were ground in a laboratory pulverizer (100 UPZ, Hosokawa Alpine, Germany), sieved through a 0.2 mm mesh, and used for aquafeed elaboration as follows: i) raw seaweed powder; ii) enzymatically hydrolysed biomass; iii) fermented biomass; and finally, iv) enzymatically hydrolysed and fermented biomass. Enzymatic hydrolysis was performed using a blend of enzymes (xylanase 20,000 Ug^{-1}; glucanase 30,000 U g^{-1}; cellulase 10,000 Ug^{-1}, and protease 10,000 U g^{-1}) at pH 5 and 50 °C during 24 h using 0.05 enzyme to substrate ratio. Fermentation of the seaweed was carried out in the fermenter vessel inoculating seaweed biomass with 10^8 CFU g^{-1} of *Saccharomyces cerevisiae* and 10^8 CFU g^{-1} of *Bacillus subtilis*. The sugar substrate dextrose was added at 5% *w*/w of the base material. The fermentation was carried out at 40 °C till the pH reached 4.5. A pH between 4 and 5 is desired for fermentation because when the pH <4, the feed intake decreases and at pH > 5, microbial spoilage is likely to occur. As detailed above, the third batch of seaweed was prepared in two sequential steps using enzymatic hydrolysis followed by fermentation. LifeBioencapsulation S.L. (Almería, Spain) generated the algal biomasses. Table 1 shows the proximal composition of the raw crude and treated algal biomasses. The chemical composition of algal biomasses and feeds was carried out according to AOAC (2000) for dry matter and ash. Crude fibre was analysed by ANKON methodology (ANKOM^{200} Fibre Analyzer, Metrohm Hispania, Madrid) following the procedure of AOAC (2000). Crude protein content (N × 6.25) was determined using elemental analysis (Fisons EA 1108 analyzer, Fisons Instruments, USA), and total lipid content was quantified according to the methods described by Folch et al. (1957). Nitrogen-free extract (Nfe) was estimated as the weight difference of crude protein, crude lipid and ash from 100, and this value was computed as the total carbohydrate content. Gross energy of the experimental diets was calculated using energetic conversion factors (16.7, 23.6 and 38.9 kJ/g for carbohydrate, protein, and lipid, respectively) according to Miglavs

Table 1
Chemical composition (% dry matter) of the different *R. okamurae* biomasses used in the feeding trial.

Algal biomass	Crude protein	Total lipids	Ash	Nfe*	Crude fibre
Crude (CR)	8.7	4.2	14.3	72.8	35.2
Hydrolysed and fermented (EF)	11.3	5.5	13.9	69.3	25.9
Hydrolysed (E)	9.0	4.9	14.9	71.2	29.0
Fermented (F)	10.1	5.3	14.1	70.5	28.5

* *Nitrogen-free extract* calculated as 100 − (% crude protein + % lipid + % ash).

and Jobling (1989).

2.3. Diets

Five grossly isoproteic, isolipidic and isoenergetic diets were formulated with a proximate composition close to commercial feeds for the European sea bass and produced at the Universidad de Almeria facilities (Experimental Aquafeed Service) using a two-screw extruder (Evolum 25, Clextral, France). Fish meal (FM), krill meal and fish oil (FO) were included at 12%, 3% and 9.2%, respectively, in all experimental diets for mimicking the dietary inclusion level of fish derivatives used these days in commercial aquafeeds for this fish species (Table 2).

This control diet (CT) was formulated without algal biomass. Each one of the four experimental and supplemented diets under study included 5% of one type of macroalgae biomasses described above: i) the crude macroalgae, without any biotechnological treatment (CR); ii) the enzymatically hydrolysed and fermented (EF), iii) the enzymatically hydrolysed (E), or iv) the fermented (F) algae biomass (Table 2). The dietary inclusion level used was chosen following a similar study carried out by Fernandes et al. (2022) in the same species using biotechnologically treated *Ulva rigida* biomass.

Table 2
Ingredient and proximate composition of the experimental diets.

Ingredient composition (% dry matter)	CT	CR	EF	E	F
Fishmeal LT94[1]	12.0	12.0	12.0	12.0	12.0
Krill meal[2]	3.0	3.0	3.0	3.0	3.0
Wheat gluten[3]	13.3	13.3	13.3	13.3	13.3
Soybean meal[4]	25.0	25.0	25.0	25.0	25.0
Soybean protein concentrate[5]	10.0	10.0	10.0	10.0	10.0
Crude algae		5.0			
Hydrolysed-fermented algae			5.00		
Hydrolysed algae				5.00	
Fermented algae					5.00
Fish oil[6]	9.2	9.2	9.2	9.2	9.2
Soybean oil[7]	4.3	4.2	4.2	4.2	4.2
Wheat meal[8]	16.5	11.6	11.6	11.6	11.6
Lysine[9]	1.5	1.5	1.5	1.5	1.5
Methionine[10]	0.6	0.6	0.6	0.6	0.6
Betain[11]	0.5	0.5	0.5	0.5	0.5
Vitamin and mineral premix[12]	2.0	2.0	2.0	2.0	2.0
Vitamin C[13]	0.1	0.1	0.1	0.1	0.1
Guar gum[14]	2.0	2.0	2.0	2.0	2.0
Proximate composition (%)					
Crude protein	43.3	43.0	42.4	42.1	42.5
Crude lipid	16.2	16.0	16.5	16.8	16.5
Ash	6.8	7.4	7.6	7.5	7.6
Gross energy (MJ/kg)[15]	22.1	22.0	22.0	22.1	22.0

Dietary codes: CT: algae-free control diet; CR stand for crude algae included at 5%. EF stand for enzymatically-hydrolysed and fermented algae included at 5%. E stand for enzymatically-hydrolysed algae included at 5%. F stand for fermented algae included at 5%.

[1] 69.4% crude protein, 12.3% crude lipid (Norsildemel, Bergen, Norway).
[2] purchased from Bacarel (UK). CPSP90 is enzymatically pre-digested fishmeal.
[3] 78% crude protein (Lorca Nutrición Animal SA, Murcia, Spain).
[4] 48% crude protein, 8% crude lipid (Lorca Nutrición Animal SA, Murcia, Spain).
[5] Soybean meal, 65% crude protein, 4% crude lipid (DSM, France).
[6] AF117DHA (Afamsa, Spain).
[7] P700IP (Lecico, DE).
[8] Local provider (Almería, Spain).
[9, 10, 11] Lorca Nutrición Animal SA (Murcia, Spain).
[12] LifeBioencapsulation S.L. (Almería, Spain). Vitamins (mg kg^{-1}): vitamin A (retinyl acetate), 2000,000 UI; vitamin D3 (DL-cholecalciferol), 200,000 UI; vitamin E (Lutavit E50), 10,000 mg; vitamin K3 (menadione sodium bisulphite), 2500 mg; vitamin B1(thiamine hydrochloride), 3000 mg; vitamin B2 (riboflavin), 3000 mg; calcium pantothenate, 10,000 mg; nicotinic acid, 20,000 mg; vitamin B6 (pyridoxine hydrochloride), 2000 mg; vitamin B9 (folic acid), 1500 mg; vitamin B12 (cyanocobalamin), 10 mg vitamin H (biotin), 300 mg; inositol, 50,000 mg; betaine (Betafin S1), 50,000 mg. Minerals (mg kg-1): Co (cobalt carbonate), 65 mg; Cu (cupric sulphate), 900 mg; Fe (iron sulphate), 600 mg; I (potassium iodide), 50 mg; Mn (manganese oxide), 960 mg; Se (sodium selenite), 1 mg; Zn (zinc sulphate) 750 mg; Ca (calcium carbonate), 18.6%; (186,000 mg); KCl, 2.41%; (24,100 mg); NaCl, 4.0% (40,000 mg).
[13] TECNOVIT, Spain;
[14] EPSA, Spain.
[15] Gross energy was estimated by energetic coefficients (kJ/g) according to Miglavs and Jobling (1989): crude protein, 23.6; crude lipid, 38.9; Nfe, 16.7.

2.4. Feeding protocol and sampling procedures

European sea bass (*D. labrax*) juveniles were obtained from commercial sources (CUPIBAR, Chiclana de la Frontera, Cádiz) and after an initial acclimation period (7 days) to the experimental facility (CTAQUA, El Puerto de Santa María, Cádiz, Spain; Spanish Operational Code REGA ES110270000411), fish were randomly distributed in fifteen 100 L tanks ($n = 20$ fish per tank, 60 fish per experimental diet, 24.6 ± 0.3 g of initial mean body weight). Tanks were coupled to a single recirculation aquaculture system (RAS), equipped with physical and biological filters, and programmable temperature (21 ± 0.5 °C) and O_2 devices (>85% saturation). The photoperiod followed the natural changes from April to July at Cádiz latitude (36°35′06"N; 06°13′48"W), and salinity maintained constant (36 ‰). The experimental diets were offered to visual satiety three times per day, six days per week, from April to July (2020). Visual satiety was established as the moment when fish lost interest in food, marked by the cessation of activity in the tank. Feed intake was recorded weekly for each replicate tank to calculate growth performance parameters.

At the end of the trial overnight fasted fish were randomly taken from each replicate tank between 9:30 and 11:00 h. This was done on three consecutive days (day 92 to day 94 of the trial), taking fish from one tank per diet daily to avoid potential circadian effects. Fish were deeply anaesthetised with an overdose of 2-phenoxyethanol (1 mL L^{-1} seawater), cervical sectioned, individually weighed, measured for standard body length, and then sampled to obtain gastrointestinal tracts.

The whole intestine was isolated and clamped (from pyloric caeca to anal sphincter) with two haemostatic forceps and then measured to obtain the Intestine length index (ILI, [100*intestine length]/standard body length). Next, 9 to 10 fish (3–4 per replicate tank) were used for electrophysiological analysis and 27–30 fish (9–10 per replicate tank) were used for intestinal fluid collection for microbiota analysis; in addition, representative biopsies from discrete regions of the intestine (anterior and posterior intestine from 3 to 4 fish per replicate tank) were also obtained for molecular analysis. The remaining fish in each tank were deeply anaesthetised in the same way, counted, and individually weighed and measured to obtain the final biomass per tank and to calculate the condition factor (K) calculated as K = (100*body weight)/fork length^3.

2.5. Intestinal electrophysiology in Ussing chambers

2.5.1. Voltage clamp

The anterior intestine was isolated and mounted as previously described (Fuentes et al., 2010) on a tissue holder of 0.25 cm^2 and positioned between two half-chambers containing 2 mL of physiological saline (147 mM NaCl, 1.1 mM $MgSO_4$, 19 mM Na-Gluconate, 3 mM KH_2PO_4, 1.5 mM $CaCl_2$, 5 mM $NaHCO_3$, 5 mM glucose, 5 mM HEPES, 5 mM Na-HEPES, with pH 7.80, Alves et al., 2019). During the ex vivo experiments, the tissue was bilaterally gassed with 0.3% CO_2 + 99.7% O_2 and at 22 °C. Short-circuit current (I_{sc}, μA cm^{-2}) was monitored by clamping the epithelia to 0 mV. Voltage clamping and current injections were performed using a VCC MC8 voltage clamp amplifier (Physiologic Instruments, San Diego, USA). Bioelectrical parameters for each tissue were recorded continuously onto Labscribe3 running in a MacIntosh computer using an IWorx188 data acquisition system from the time of mounting for 90 min. Epithelial resistance (Rt, Ω.cm^2) was manually calculated (Ohm's law) using the current deflections induced by a

bilateral ±1 mV pulse of 3 s every minute. The apical side of the preparation was considered as the ground. Therefore, positive currents are absorptive, while secretory currents are negative.

2.5.2. Permeability assay

After 20–30 min of tissue stabilisation after mounting in vitro, the saline was replaced with a fresh well-gassed solution to a final volume of 1.2 mL per chamber, and a permeability assay was carried out as described in Molina-Roque et al. (2022), adapted for fish from Arnold et al. (2019). In short, enough fluorescein isothiocyanate–dextran (FITC, average mol. wt. 4000, Sigma, Madrid) and Rhodamine B isothiocyanate–dextran (RITC, average mol. wt. 70,000, Sigma, Madrid) prepared as concentrated stocks of 100 mg mL^{-1} were added to final concentrations of 0.5 mg mL^{-1} to the apical chamber and a sample (0.2 mL) collected from both the apical and the basolateral compartments after 15 min of mixing to establish time zero. After exactly 1-h, new samples from both the donor and receiver compartments were collected into fresh vials.

Fluorescence measurements were performed using a Multi-Mode Microplate Reader BioTek SynergyTM 4 (BioTek® Instruments, Winooski, VT, USA) set for excitation wavelength at 492 nm and emission wavelength at 520 nm for FITC and set for excitation wavelength at 530 nm and emission wavelength at 590 nm for RITC. To establish concentrations in the apical and basolateral chambers, we used standards in the range of 0.2–2000 ng.

The apparent permeability (P_{app}) was estimated using the equation: $P_{app} = (V*dC)/(A*C_0*dT)$, where P_{app} is the permeability in centimetres per second, V is the volume of the receiver chamber, A is the surface area of the tissue in square centimetres, C_0 is the starting concentration in the donor compartment (apical) and dC/dT is the rate of concentration change (ng s^{-1}) of FITC and RITC in the receiving chamber (basolateral).

2.6. Microbiota analysis

2.6.1. DNA extraction

The procedure was done in a flow cabinet, on an ice tray covered with a fresh disposable sterile cloth and using fresh disposable sterile dissecting tools for each fish. After intestinal clamping (as described in Section 2.4.), the intestinal fluid was collected into a sterile vial for DNA extraction. Bacterial DNA extraction was conducted in fresh intestinal fluid samples immediately after collecting, using the EZNA stool DNA kit (Omega Bio-Tek, United States) following the manufacturer's instructions in the Pathogen Detection Protocol. For each extraction sample, the intestinal fluid of three animals was combined using equal volumes. A total of 3 extraction samples per tank ($n = 9$ fish/tank), from 3 tanks per treatment (n = 9 DNA samples/experimental diet from 27 fish), were processed. After extraction, DNA was stored at −20 °C until used.

2.6.2. Library construction, verification and NGS sequencing

Before sequencing, DNA samples were analysed in-house to ensure samples had sufficient integrity and quantity (at least 10 ng μL^{-1}) for optimal amplification. Each DNA sample was quantified using the Qubit® 2.0 fluorometer and the Qubit™ dsDNA BR Assay Kit (Thermo Fisher Scientific), following the manufacturer's instructions. Quality was verified through 1.5% agarose gel electrophoresis using 1 μL of each DNA sample. Next, samples were commercially sequenced at Stab Vida, Lda. (Caparica, Portugal). The NGS sequencing project started with library construction (region V3-V4 of the 16S RNA gene, reference nucleotide interval 341–805 nt) for each DNA sample, performed using the Illumina 16S Metagenomic Sequencing Library preparation protocol. Ten ng of each DNA sample were used for the first PCR round, with KAPA HiFi HotStart ReadyMix and 200 nM of primers, in a final reaction volume of 25 μL. The gene-specific primers used in this protocol were taken from Klindworth et al. (2013) as the most promising primer pair: Forward Primer (5′- CCTACGGGNGGCWGCAG-3′) and Reverse Primer (5′-GACTACHVGGGTATCTAATCC-3′). Illumina adapter overhang nucleotide sequences were added to the gene-specific primer sequences: Forward overhang (5′- TCGTCGGCAGCGTCAGATGTGTATAAGAGACAG-3′) and Reverse overhang (5′-GTCTCGTGGGCTCGGAGATGTGTATAAGAGACAG-3′). Cycling conditions were an initial step at 95 °C for 3 min, followed by 25 cycles of 95 °C for 30 s, 55 °C for 30 s, 72 °C for 30 s, ending with a final extension step at 72 °C for 5 min. After this first PCR, products in each library were checked on a Bioanalyzer DNA 1000 chip (Agilent) to verify the size. Next, libraries from each treatment were pooled, i.e., 9 libraries per treatment (3 per replicate tank) were combined and purified using AMPure XP beads (Beckman Coulter, Life Sciences). Five μL of each pooled library was subjected to a second PCR (index PCR) to attach dual indices and Illumina sequencing adapters using the Nextera XT Index kit and KAPA HiFi HotStart ReadyMix, in a 50 μL reaction volume. Cycling conditions were the same as in the first round except that only 8 cycles were used. Another cleaning step with AMPure XP beads (Beckman Coulter, Life Sciences) was performed to clean up the final libraries before quantification with the Qubit® 2.0 fluorometer and the Qubit™ dsDNA BR Assay Kit (Thermo Fisher Scientific).

After verifying that all re-amplifications had reached a concentration above the 4 nM threshold, the DNA fragments were sequenced with MiSeq Reagent Kit v3 in the lllumina MiSeq platform, using 300 bp paired-end sequencing reads.

2.6.3. Bioinformatic analyses and data curation

The quality of the produced data was determined by Phred quality score at each cycle (position in the read). The plot containing the average quality at each cycle was created with the FastQC tool (Andrews, 2010) The analysis of the generated raw sequence data, feature table construction, and taxonomy classifications were conducted using QIIME2 v2020.8 (Caporaso et al., 2010).

The reads were denoised using the DADA2 plugin (Callahan et al., 2016). The following processes were applied: trimming and truncating low-quality regions, dereplicating the reads, and filtering chimaeras.

In the case of species diversity analysis, it is necessary to know whether the number of reads of the sequencing reaches a reasonable amount so that more sequencing does not significantly increase species diversity. We randomly selected a different number of sequences and analysed the operational taxonomic units (OTUs) detected at each fraction to form a rarefaction curve. The reads were organized in OTUs and then classified by taxon using a fitted classifier. The scikit-learn classifier was used to train the classifier using the SILVA database. For classification purposes, only OTUs containing at least 10 sequence reads were considered significant.

This Targeted Locus Study project (PID PRJNA860562) has been deposited at DDBJ/EMBL/GenBank under the accession KFVS00000000. The version described in this paper is the first version, KFVS01000000.

2.7. Expression analysis

2.7.1. Sample collection and RNA extraction

Upon intestinal dissection, anterior and posterior intestinal tissue samples were immediately taken, submerged in >10 volumes of RNAlater® (Sigma-Aldrich) and kept at −20 °C until RNA extraction. Three to four animals per tank from triplicate tanks per treatment were sampled, in a total of at least 9 animals per treatment and the corresponding 9 tissue samples per intestinal region.

Total RNA was isolated using the NucleoSpin® RNA kit, from Macherey-Nagel, following the manufacturer's instructions. Then, RNA was quantified for each sample using the Qubit™ RNA BR Assay Kit from Invitrogen. The quality (RIN) of each RNA sample was verified using the Agilent 2100 Bioanalyzer and the RNA Nano Kit from Agilent technologies. Only samples with RIN higher than 8.5, which is indicative of clean and intact RNA, were used for further analysis.

2.7.2. Primer design and qPCR analysis

Primers were designed for each gene of interest with the software Primer3 (v. 0.4.0) (Koressaar and Remm, 2007; Untergasser et al., 2012), either using sequences retrieved from the GenBank or using sequences previously generated from RNAseq (Fuentes Lab, Supplementary Table S1).

First-strand cDNA of each sample was synthesized from 1 μg total RNA using the High-Capacity cDNA Reverse Transcription Kit (Applied Biosystems, USA) according to the user's manual.

qPCR was performed using iQ™ SYBR® Green Supermix (Bio-Rad, USA) in a CFX Touch™ Real-Time PCR Detection System (Bio-Rad, USA). A volume of 10 μL with 0.4 μM of each primer (Supplementary Table S1), 2 μL of cDNA (10 ng of cDNA assumed from RNA input), 2.6 μL of MQ water and 5 μL of 2× iQ SYBR Green Supermix was used for each qPCR reaction. Cycling conditions were an initial denaturation for 5 min at 95 °C, followed by 40 cycles of 15 s at 95 °C and 30 s at 60 °C. A melting curve analysis ensued after completion of the 40 cycles to verify no non-specific amplification was obtained. The reference genes *actb* and *eef1a* were used for normalization. Transcripts quantification was performed according to the Pfaffl method (Pfaffl, 2001) and corrected for the efficiency of each primer pair. All the R^2 from the calibration plots were in the range of 0.980 and 1. Values were expressed as fold change calculated in relation to values of the control group after normalization against those of the reference genes. At least nine biological replicates with two technical replicates each were used for the qPCR analyses.

2.8. Statistical analyses

All results are shown as mean ± standard error of the mean (mean ± SEM). After verifying homogeneity of variance and normality, statistical analysis of the data was conducted by using One-Way analysis of variance (ANOVA) followed by Dunnett's multiple comparisons test performed with GraphPad Prism version 9.3.1 for macOS (GraphPad Software, San Diego, California USA, www.graphpad.com). A comparison of triplicate tanks for all parameters was also performed with One-Way ANOVA. The level of significance was set at $p < 0.05$.

For estimates of alpha diversity in the microbiota samples, a hit map (number of reads allocated to each OTU at Class level) was imported to PRIMER-e, version 7 software (Massey University, Albany, New Zealand), with the PERMANOVA + add-on (Clarke et al., 2014), and diversity indexes (Chao, Shannon–Weaver and Simpson reciprocal) were calculated for each combined sample.

To explore the variance in microbial communities between diets and test beta diversity, a multivariate analysis was conducted using the microbiota relative frequency values. Data were square-root transformed and the Bray-Curtis dissimilarity coefficient was used to construct a resemblance matrix, prior to subsequent analyses: CLUSTER, SIMPROF (Similarity Profile Analysis) and Monte Carlo test, with data visualized using Principal Coordinate (PCO) analysis. A SIMPER (Similarity percentages) analysis was used to identify which OTUs were mainly responding to the different diets under evaluation.

In addition, multivariate analyses were conducted separately in the anterior and posterior intestine gene expression data sets. Both data sets were square-root transformed, and a Bray-Curtis dissimilarity coefficient was used to construct resemblance matrices prior to subsequent analyses: ANOSIM (Analysis of Similarities, One-Way A), SIMPROF, SIMPER and PERMANOVA (Permutational Multivariate Analysis of Variance).

To further explore the effect of each diet on the expression level of immune-related genes in each intestinal region, the Bray-Curtis dissimilarity coefficient was used to construct a resemblance matrix. A PERMANOVA analysis (pair-wise tests) was run on that resemblance matrix, and a multivariate means plot (e.g., a representation of the average effect of each diet on gene expression level at each intestinal region), together with an approximate measure of the uncertainty about those means, were calculated using the routine Bootstrap averages and visualized using metric multidimensional scaling analysis (MDS).

3. Results

3.1. Growth performance and biometric parameters

No mortality occurred during the experiment, and animals grew from 24.6 ± 0.3 g of initial body mass to 65–77 g, depending on the dietary group. Significant differences in the body weight were observed at the end of the experiment, with a reduction in diets including crude (CR), enzymatically treated (E) or fermented (F) algae biomass, though not in the enzymatically hydrolysed and fermented (EF) diet, when compared to the control (CT) group. The same pattern was observed for SGR, where CR, E and F diets caused a significant decrease in relation to CT, not seen with the EF diet. No differences were observed in feed intake (g aquafeed/fish), but a significant increase of FCR was observed in fish fed CR diet compared to those of the CT group. In contrast, the other diets did not significantly alter FCR when compared to CT. In addition, CT group showed the highest final fork length, being significantly different compared to both CR and F groups, but not EF and E groups. This result reveals differentiated growth potential among treatments, albeit without significant variation in the condition factor (K). Finally, we observed an evident elongation of the intestine of fish fed CR diet, causing a significant increase in the ILI (%) somatic index when compared with the CT group. In contrast, fish from the EF group showed a significantly lower ILI value than the CT (Table 3).

3.2. Tissue resistance and permeability in Ussing chambers

Electrophysiological analysis of the intestine showed a significant decrease in the epithelial resistance (R_t) of fish fed with the four supplemented diets (CR, EF, E, F) when compared to the CT group (Fig. 1A), whereas a significant increase in the short-circuit current (I_{sc}) was only

Table 3
Growth performance and somatic indexes of European sea bass juveniles fed to visual satiety the experimental diets over 92 days with a control aquafeed and four supplemented diets with 5% of different *R. okamurae* products. Data on biometric parameters are the mean ± SEM of 60 fish/diet.

	CT	CR	EF	E	F
Initial body mass (g)	25.78 ± 0.17	25.85 ± 0.18	25.71 ± 0.19	25.99 ± 0.19	25.76 ± 0.17
Final body mass (g)	77.51 ± 1.29	65.34 ± 3.18**	74.24 ± 0.44	67.59 ± 2.63*	66.51 ± 0.86**
Final fork length (cm)	19.0 ± 0.2	18.0 ± 0.2*	18.4 ± 0.3	18.3 ± 0.2	18.2 ± 0.2*
SGR[a]	1.21 ± 0.03	1.01 ± 0.05**	1.17 ± 0.02	1.08 ± 0.01*	1.05 ± 0.01*
K[b]	1.11 ± 0.01	1.06 ± 0.02	1.09 ± 0.02	1.06 ± 0.02	1.06 ± 0.02
Feed intake (g/fish)	72.5 ± 1.6	63.9 ± 5.6	72.7 ± 3.7	67.0 ± 1.2	63.2 ± 3.9
FCR[c]	1.40 ± 0.02	1.61 ± 0.03*	1.47 ± 0.03	1.55 ± 0.02	1.53 ± 0.04
ILI (%)[d]	59.97 ± 2.83	66.33 ± 1.31*	47.14 ± 2.13**	56.10 ± 2.11	55.15 ± 2.90

Data on biometric parameters are the mean ± SEM of 60 fish/diet. Data on somatic indexes are the mean ± SEM of 12 fish/diet. Data on SGR, FCR and Feed intake are the mean ± SEM of triplicate tanks per diet. Asterisks indicate significant differences among dietary treatments versus the control (CT) group based on one-way ANOVA and Dunnett's test (*$p < 0.05$; **$p < 0.01$). CT: control; CR: crude macroalgae; EF: enzymatically hydrolysed and fermented biomass; E: enzymatically hydrolysed biomass; F: fermented biomass.

[a] Specific growth rate = 100 * (ln final body weight − ln initial body weight)/days.

[b] Condition factor = (100*body weight)/fork length^3.

[c] Feed Conversion Ratio = (100*total feed intake)/total weight gain.

[d] Intestine length index = (100*intestine length)/fork length.

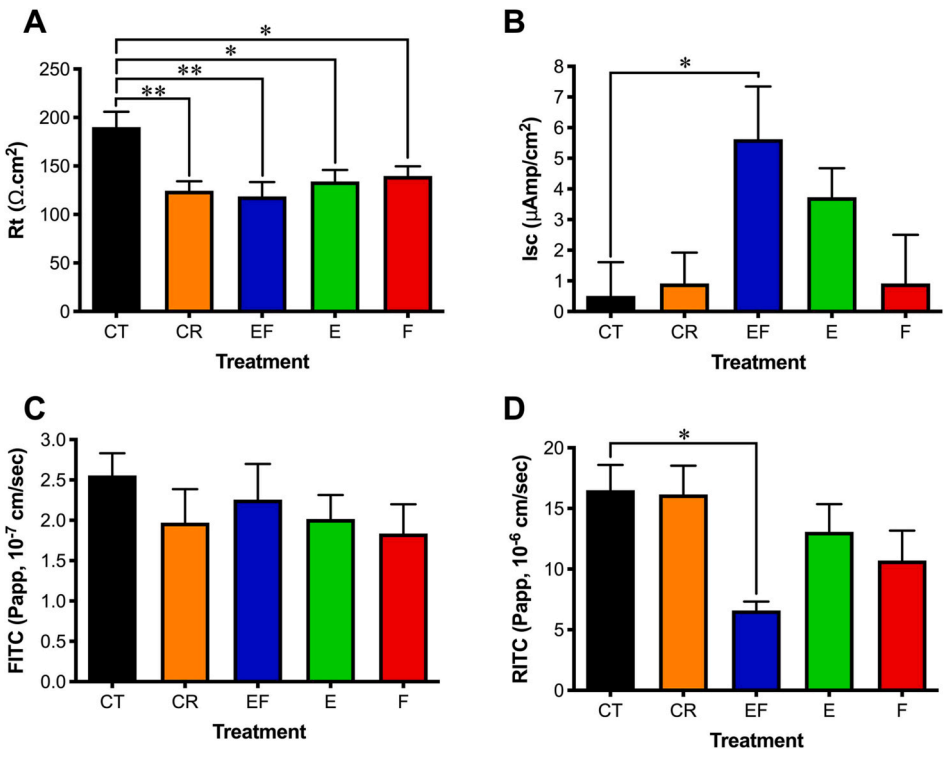

Fig. 1. Basal transepithelial resistance (A, R_t, Ω cm^2), basal short circuit current (B, I_{sc}, µA cm^{-2}), apparent permeability (C, 10^{-7}*P_{app}, cm s^{-1}) to FITC dextran (4 kD) and apparent permeability (D, 10^{-6} *P_{app}, cm s^{-1}) to RITC dextran (70 kD) in the anterior intestine of European sea bass (*D. labrax* L.) fed the experimental diets over 92 days. CT – Control diet; CR – diet with crude algae biomass; EF – diet with enzymatically hydrolysed and fermented algae biomass; E – diet with enzymatically hydrolysed algae biomass; F- diet with fermented algae biomass. Each column represents the average + SEM (n = 10). Significant differences versus control obtained in a One-Way ANOVA with Dunnett's multiple comparisons test are indicated as *$p < 0.05$ or **for $p < 0.01$.

observed in the EF experimental group (Fig. 1B). Regarding intestinal permeability (P_{app}), FITC did not show differences among experimental groups (Fig. 1C), although RITC revealed a significant reduction in the EF group when compared with fish fed the CT diet (Fig. 1D).

3.3. Microbiota analysis

3.3.1. Sequencing depth

The intestinal microbiota composition for each treatment was analysed by sequencing a fragment of the V3-V4 hypervariable region of the 16S rRNA gene. After filtering as described in Section 2.6.3), a maximum of 394,102 reads (for CT) and a minimum of 289,822 reads (for E) were obtained. These 300 bp sequences were assigned to 541 unique features (OTUs) based on 97% similarity using QIIME, and a taxonomical classification was performed using the SILVA database. Rarefaction curves reached the saturation phase between 10,000 and 20,000 sequence readings (Supplementary Fig. S1).

3.3.2. Diversity analysis of microbiota in the five pooled samples

The alpha diversity indexes were found highest for the microbiota of the CR group and lowest for the F group (Supplementary Table S2), with samples of fish fed CT, E and EF diets having very similar values in all calculated indexes.

Beta diversity analyses are illustrated as CLUSTER and principal coordinates (PCO) plots in Supplementary Figs. S2 and S3, respectively. Both analyses show significant differentiation between the bacterial community of the samples pooled from animals under the F diet and the bacterial communities observed in the samples pooled from the other diets (SIMPROF Type 1 test, $p < 5\%$; Monte-Carlo test $P = 0.048$). With a simple experimental design such as the present, the number of possible permutations is not sufficient for a proper PERMANOVA analysis, and instead, the Monte Carlo test should be used (Clarke et al., 2014), as was done here.

3.3.3. Composition of microbial communities

There was a 2.64% relative frequency of unassigned OTUs in the case of the fish fed CR diet, but this value was below 0.4% in all other treatments. The taxonomic compositions of *D. labrax* intestinal microbiota primarily presented representatives of the phyla Proteobacteria and Bacteroidota, followed by Patescibacteria, Verrucomicrobiota, Actinobacteria and Firmicutes (Fig. 2 and Supplementary Table S3). A marked decrease in the relative frequency of phyla Proteobacteria and Bacteroidota was observed in the E and F groups compared to fish fed the other three diets. However, marked differences in the relative frequency of families within each phylum were also observed, depending on the diet (Supplementary Table S4). In the fish fed CT diet, the family *Flavobacteriaceae* comprised 41.65% of the Bacteroidota and Proteobacteria were mainly represented by the *Rhodobacteraceae* (36%), with only 1.3% ascribed to the *Vibrionaceae* family. In contrast, in all other dietary groups, the relative frequency for *Vibrionaceae* was higher than 20%, reaching 50% and 84%, respectively, in the fish fed E and the F diets. Although the relative frequency of the *Flavobacteriaceae* family systematically decreased in all other groups compared to the CT, it reached the lowest value in F. The same effect was observed for the *Rhodobacteraceae* family. Other than for these three families (*Vibrionaceae, Flavobacteriaceae* and *Rhodobacteraceae*), the relative frequency values found in the fish fed F diet were equal to or below 1%. These differences were further highlighted in the SIMPER analysis (similarity percentages – species contributions, One-Way analysis; Supplementary Table S5). The average dissimilarity between the fish fed F diet and the group composed by all the other samples was 32.39%, whereas the similarity between samples from the same cluster was 81.98%. This analysis also revealed that the main OTUs driving the difference between the two groups were Gammaproteobacteria (34.07%), Alphaproteobacteria (18.13%) and Bacteroidia (16.11%). This information was overlaid onto the result of the PCO analysis (Supplementary Fig. S3).

3.4. Gene expression analysis

3.4.1. Epithelial integrity

The expression of 9 genes coding for proteins involved in maintaining the structural integrity of the intestinal epithelium was analysed

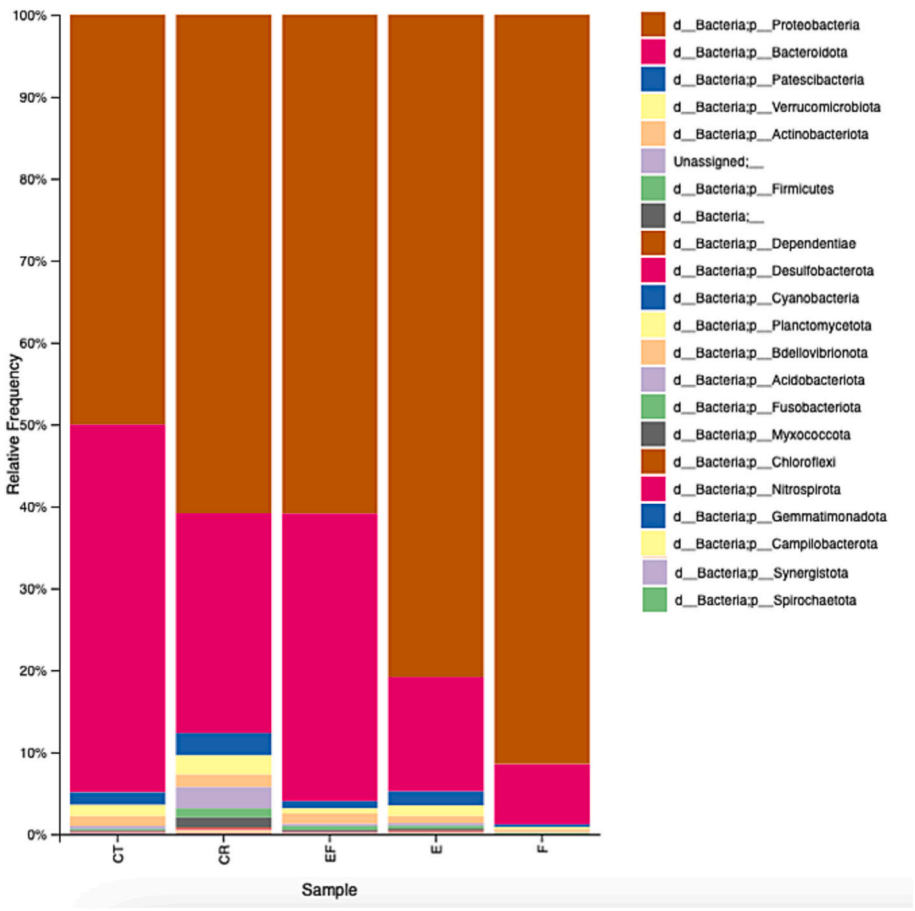

Fig. 2. Relative frequency (%) at the phylum level for each pooled sample of microbiota from the intestinal fluid of European sea bass (*D. labrax* L.) fed the experimental diets over 92 days. CT – Control diet; CR – diet with crude algae biomass; EF – diet with enzymatically hydrolysed and fermented algae biomass; E – diet with enzymatically hydrolysed algae biomass; F- diet with fermented algae biomass.

in the anterior intestine (Supplementary Table S1, Fig. 3). Only in four of those genes the expression was found to be altered in relation to the CT diet, by showing a significant decrease in the expression fold change: *cdh17* in all dietary groups, *cldn 15* in the CR, E and F groups, *tjap* in the CR and E groups, and *jama* in the CR group.

3.4.2. Amino-acid transport and metabolism

For this panel, the expression of eight genes was analysed in the anterior intestine. We included three solute carrier transporters from the Slc6a family and two from the Slc38a family, as well as *alpi*, *anpep* and *si*. A significant decrease in fold change was observed in the case of the *slc38a2*, in all dietary groups except in the F group, and in the case of *slc6a16a* in the fish fed CR and E diets. For all other 6 genes tested, no significant changes in expression were detected (Supplementary Table S1, Fig. 4).

3.4.3. Immune response

The expression levels of nine immune-related genes (Supplementary Table S1) were analysed in samples from the anterior and the posterior intestine for all diets. Only the expression of gene *il6* was found to be significantly affected (up-regulated) in relation to CT in the anterior intestine and only in the EF group (Fig. 5). In contrast, in the posterior intestine, the expression level of *il6* was not significantly affected. However, in this region, the expression levels of *ifng* and *il10* were significantly increased in the fish fed EF and F diets, whereas the transcripts of *il8* and *il12b* showed a significant increase in the CR group (Fig. 6.)

3.4.4. Multivariate analysis

In the anterior intestine, the ANOSIM (Analysis of Similarities, One-Way A) run on the resemblance matrix (S17 Bray-Curtis similarity) did not find statistically significant differences in the five diets in terms of their overall effect on the expression of all genes under analysis. However, a PERMANOVA analysis (pair-wise tests) run on the same resemblance matrix showed a significant difference between the CT and the CR diets ($P = 0.042$), but not for any other pair-wise test. The SIMPER (Similarity Percentages) analysis (Supplementary Table S6) run on the square-root transformed data matrix found the highest and lowest average similarity, respectively, in groups F (90.53) and CT (87.05) with the highest average dissimilarity between groups CT and CR (12.41) and the lowest average dissimilarity between groups EF and F (9.98). Taken together these data suggest that, in the anterior intestine, only the CR diet significantly affected the expression pattern of the genes analysed.

In the posterior intestine, the ANOSIM run on the resemblance matrix (S17 Bray-Curtis similarity) did not find statistically significant differences in the five diets regarding their overall effect on the expression of the immune-related genes under analysis. However, a PERMANOVA analysis (pair-wise tests) run on the same resemblance matrix showed a significant difference between the CT diet and the EF ($P = 0.037$) and F ($P = 0.003$) diets, and between the E diet and EF ($P = 0.033$) and F ($P = 0.001$) diets. No significant differences were found for any other pair-wise test. The SIMPER (Similarity Percentages) analysis (Supplementary Table S7) run on the square-root transformed data matrix found the highest and lowest average similarity, respectively, in groups EF (87.75) and CR (84.73) with the highest average dissimilarity between groups CR and F (15.45) and the lowest average dissimilarity

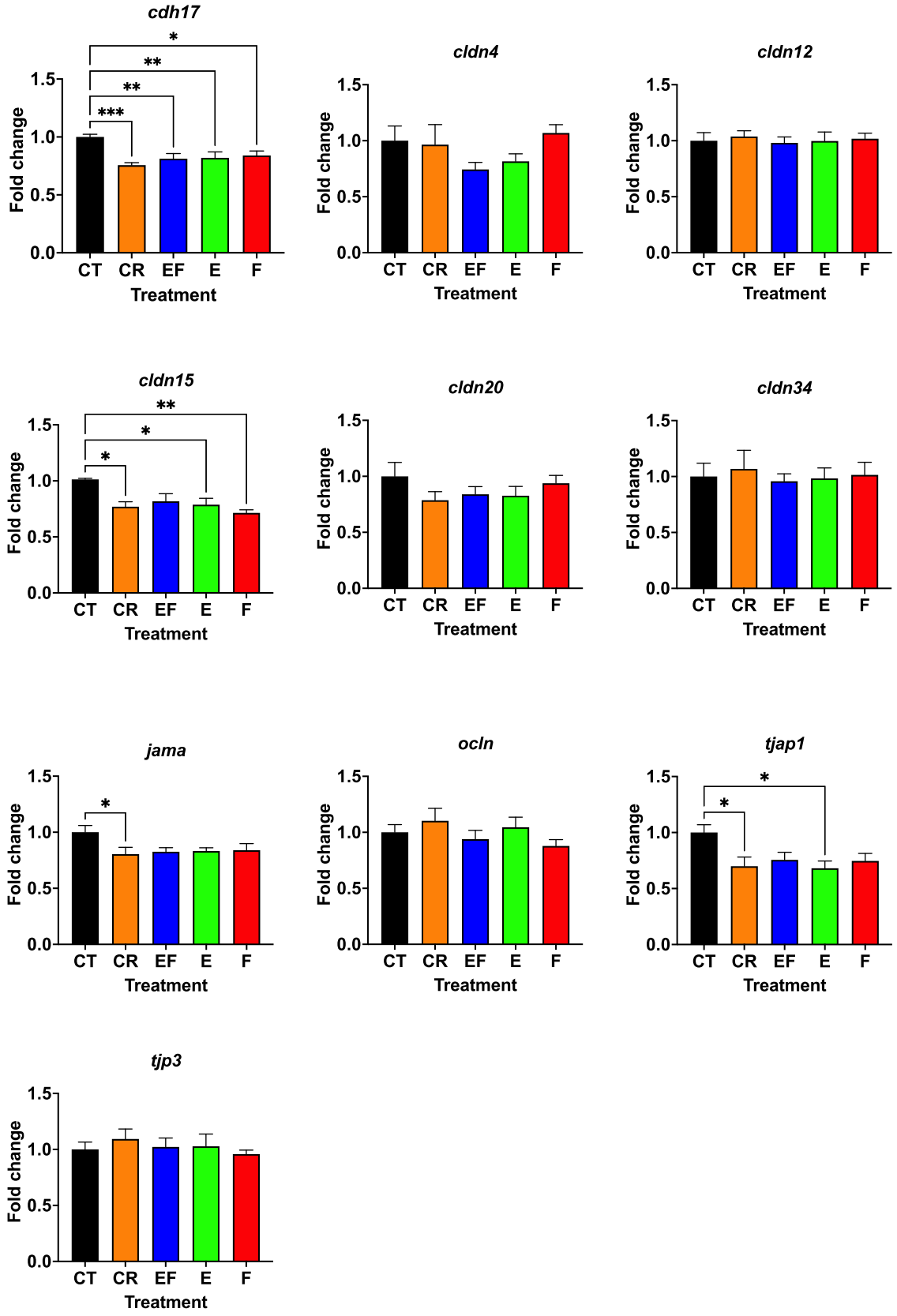

Fig. 3. qPCR results for the epithelium integrity-related genes analysed in the anterior intestine of European sea bass (*D. labrax* L.) fed the experimental diets over 92 days. CT – Control diet; CR – diet with crude algae biomass; EF – diet with enzymatically hydrolysed and fermented algae biomass; E – diet with enzymatically hydrolysed algae biomass; F- diet with fermented algae biomass. Values were expressed as fold change calculated in relation to values of the control group, after normalization against those of the reference genes. Significant differences versus control obtained in a One-Way ANOVA with Dunnett's multiple comparisons test are indicated as $*p < 0.05$, $**p < 0.01$ or $**p < 0.001$.

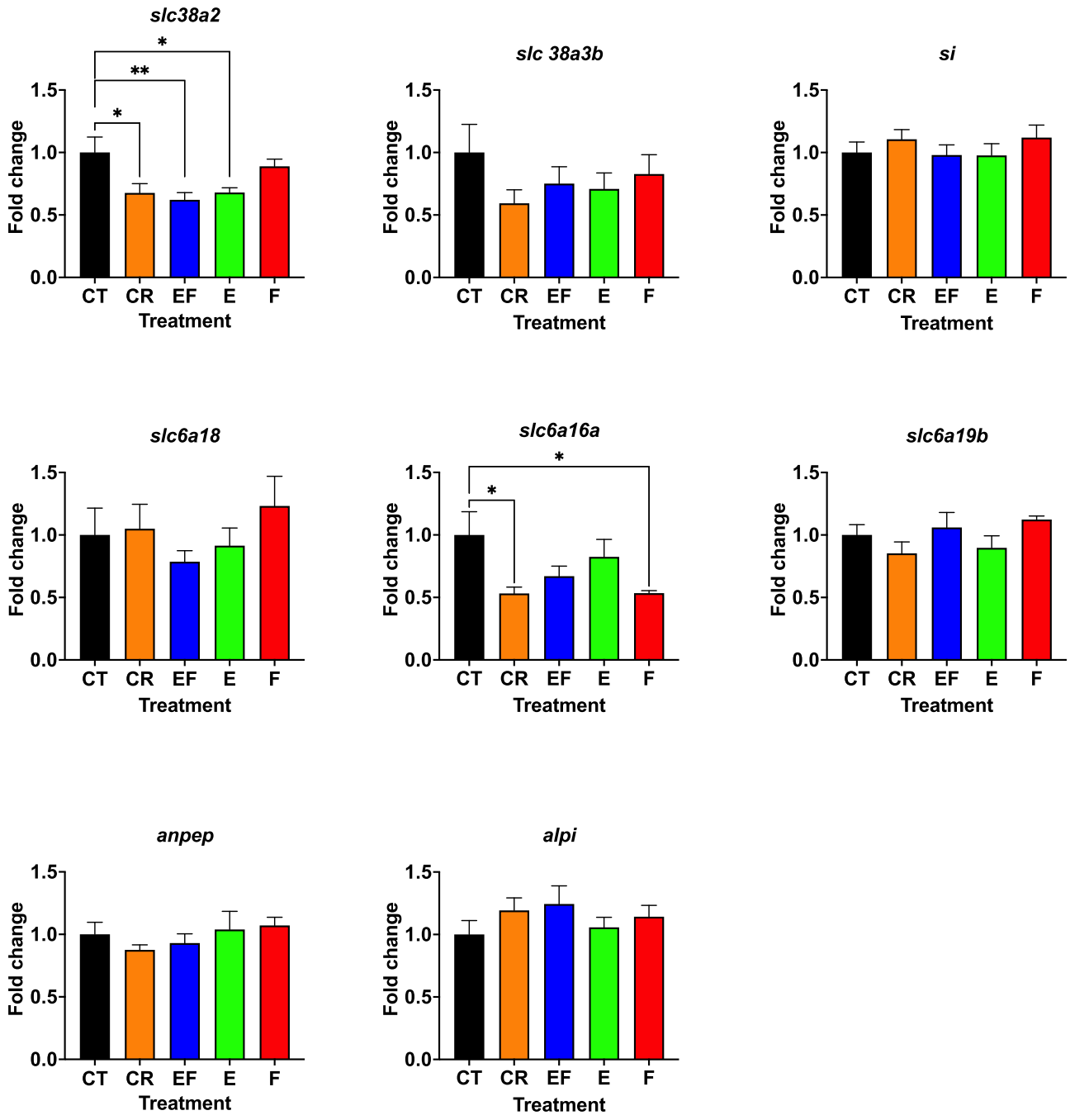

Fig. 4. qPCR results for the amino-acid transport- and metabolism-related genes analysed in the anterior intestine of European sea bass (*D. labrax* L.) fed the experimental diets over 92 days. CT – Control diet; CR – diet with crude algae biomass; EF – diet with enzymatically hydrolysed and fermented algae biomass; E – diet with enzymatically hydrolysed algae biomass; F- diet with fermented algae biomass. Values were expressed as fold change calculated in relation to values of the control group, after normalization against those of the reference genes. Significant differences versus control obtained in a One-Way ANOVA with Dunnett's multiple comparisons test are indicated as $*p < 0.05$, $**p < 0.01$ or $**p < 0.001$.

between groups CT and E (12.56).

To further test the statistical significance of the observed differences in expression levels of immune-related genes between the anterior and posterior intestinal regions in the CR, EF, E and F diets, a multivariate means plot was obtained by running the routine Bootstrap averages in PRIMER-e on the resemblance matrix. Fig. 7 shows the MDS plot of group averages and confidence limits of the effect of each of those four diets on the expression of immune-related genes in each intestinal region. A PERMANOVA analysis (pair-wise tests) run on the same resemblance matrix further supported the statistical significance of different immune-related responses observed between the anterior and posterior intestinal regions in the CR ($P = 0.003$), EF ($P = 0.004$) and the F ($P = 0.016$) diets. As expected, no significant difference between anterior and posterior intestine immune responses was detected in the E diet ($P = 0.357$).

4. Discussion

We set out this study to test whether the inclusion of *R. okamurae* biomass, an invasive seaweed on the coast of the Mediterranean Sea and

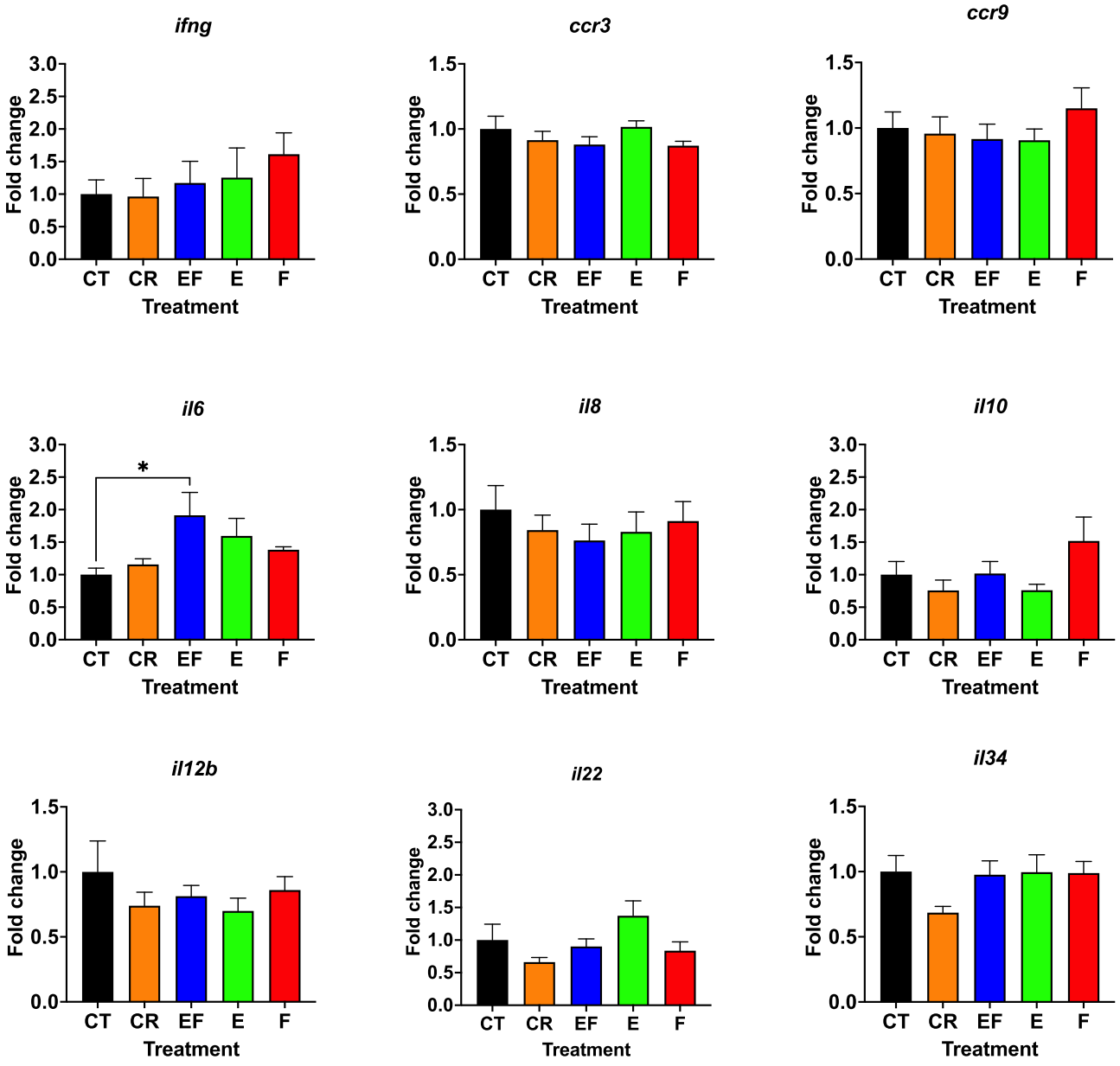

Fig. 5. qPCR results for the immune-related genes analysed in the anterior intestine of European sea bass (*D. labrax* L.) fed the experimental diets over 92 days. CT – Control diet; CR – diet with crude algae biomass; EF – diet with enzymatically hydrolysed and fermented algae biomass; E – diet with enzymatically hydrolysed algae biomass; F- diet with fermented algae biomass. Values were expressed as fold change calculated in relation to values of the control group, after normalization against those of the reference genes. Significant differences versus control obtained in a One-Way ANOVA with Dunnett's multiple comparisons test are indicated as $*p < 0.05$, $**p < 0.01$ or $**p < 0.001$.

the Atlantic Ocean, could be used as ingredient to replace some of the ingredients in aquafeeds for European sea bass. To this end, we prepared four experimental diets in which the wheat meal of the control diet (CT) was partially replaced (5% w:w) by *R. okamurae* biomass, either crude (CR), enzymatically hydrolysed and fermented (EF), hydrolysed (E) or fermented (F).

The focus of our work was on the intestine and on intestinal responses to feed composition manipulation. We first identified impacts on growth performance and somatic indexes, which did not seem to be directly affected by feed intake, but by a reduction of nutrient assimilation and/or conversion as suggested by the values of SGR and FCR. Overall, the groups fed CR and F diets resulted in smaller (shorter and lighter) animals with longer intestines in the case of CR. The animals fed the E diet were lighter, while the effect of the EF diet was only significant in the intestine length (smaller ILI than CT). The contrasting impact on the intestinal length caused by the CR and EF diets is a striking alteration in morphology since it is well-known in fish that diet correlates with digestive ability (Serra et al., 2021).

Having established significant morphometric changes, we aimed to expose putative intestine functional alterations in response to the inclusion of *R. okamurae* in the diet. Previous work documented that vegetable protein in fish feeds, such as the inclusion of different amounts of microalgae, can compromise or alter intestinal function or integrity, at least in the Gilthead sea bream (Estensoro et al., 2016; Molina-Roque et al., 2022). Therefore, we measured tissue resistance (Rt) in Ussing chambers, which is the gold standard for exposing tissue integrity and

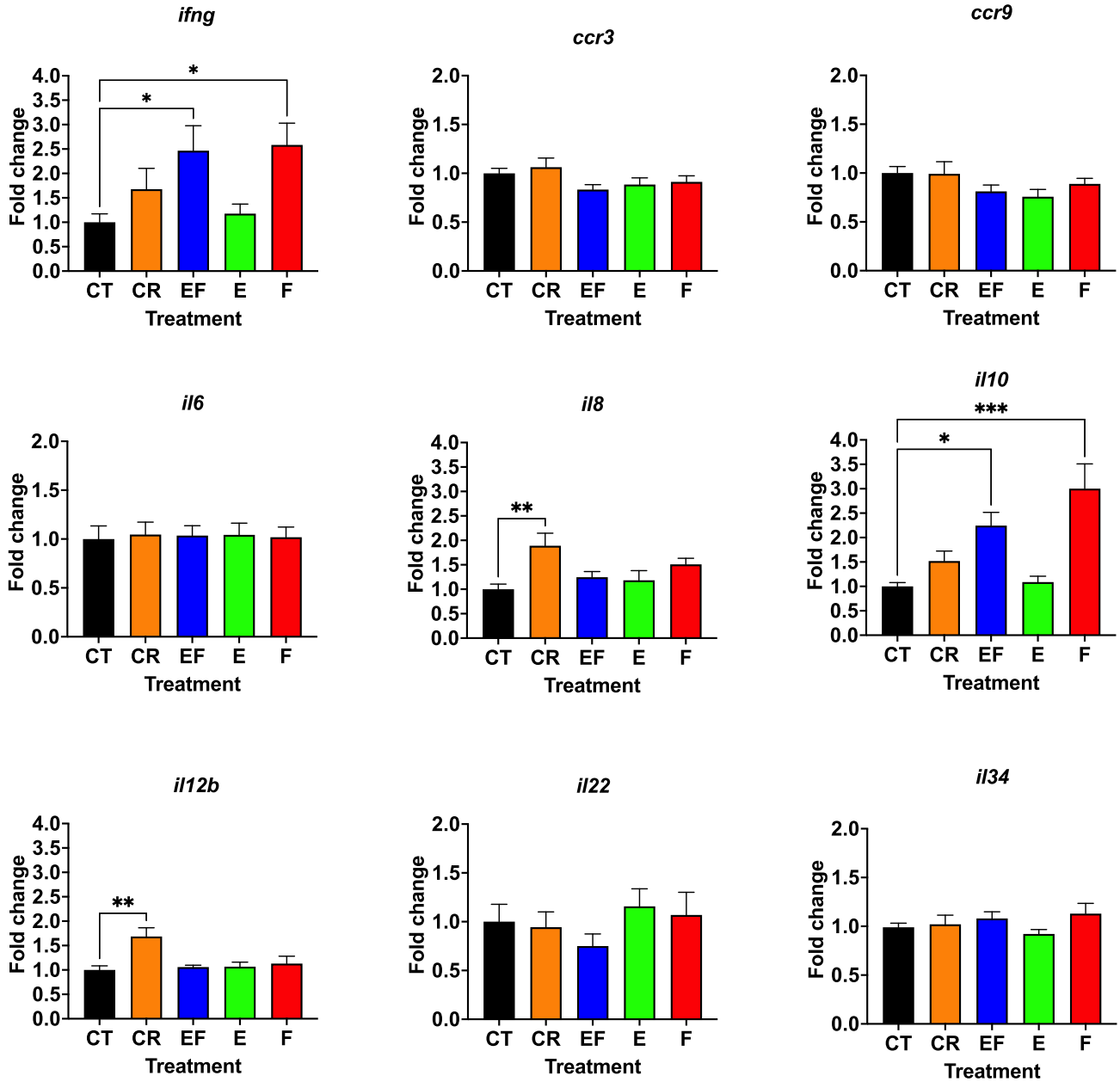

Fig. 6. qPCR results for the immune-related genes analysed in the posterior intestine of European sea bass (*D. labrax* L.) fed the experimental diets over 92 days. CT – Control diet; CR – diet with crude algae biomass; EF – diet with enzymatically hydrolysed and fermented algae biomass; E – diet with enzymatically hydrolysed algae biomass; F- diet with fermented algae biomass. Values were expressed as fold change calculated in relation to values of the control group, after normalization against those of the reference genes. Significant differences versus control obtained in a One-Way ANOVA with Dunnett's multiple comparisons test are indicated as $*p < 0.05$, $**p < 0.01$ or $**p < 0.001$.

selectivity changes. In our study in the sea bass intestine, the resistance of the epithelium significantly decreased to similar values in all diets compared to control fish (CT group). This decrease reveals intestinal barrier function modifications and epithelial integrity impairment. To further consolidate our results, we measured paracellular permeability using standard methods with 4kD FITC-dextran (Balda et al., 1996) and 70 kD RITC-dextran. The permeability of the epithelium to relatively small molecules (FITC, 4 kD) was unaffected. Still, a significantly reduced permeability to larger molecules (RITC, 70 kD) was observed in fish fed the EF formulation. Additionally, we tested the expression of an array of putative markers of epithelial integrity (Van Itallie and Anderson, 2014), such as cadherins (*cdh17*), claudins (*cldn4*, *12*, *15*, *20* and *34*), occludin (*ocln*), tight junction proteins or tight junction-associated proteins (*tjp3* and *tjap1*), and junctional adhesion molecule-A (*jama*). Most genes showed no response to dietary manipulation in relation to the CT diet. Nevertheless, the significant changes found in gene expression showed a consistent downregulation effect compared to CT values, supporting the dietary impact of feed manipulation in sea bass intestinal barrier function, already shown by the decrease in Rt. This effect was particularly evident with *cdh17* and *cldn15,* which will likely serve as molecular markers for the diagnosis of epithelial integrity together with tissue resistance measurements.

To further evaluate other possible diet-induced changes in digestive-absorptive processes, we also analysed the gene expression levels of

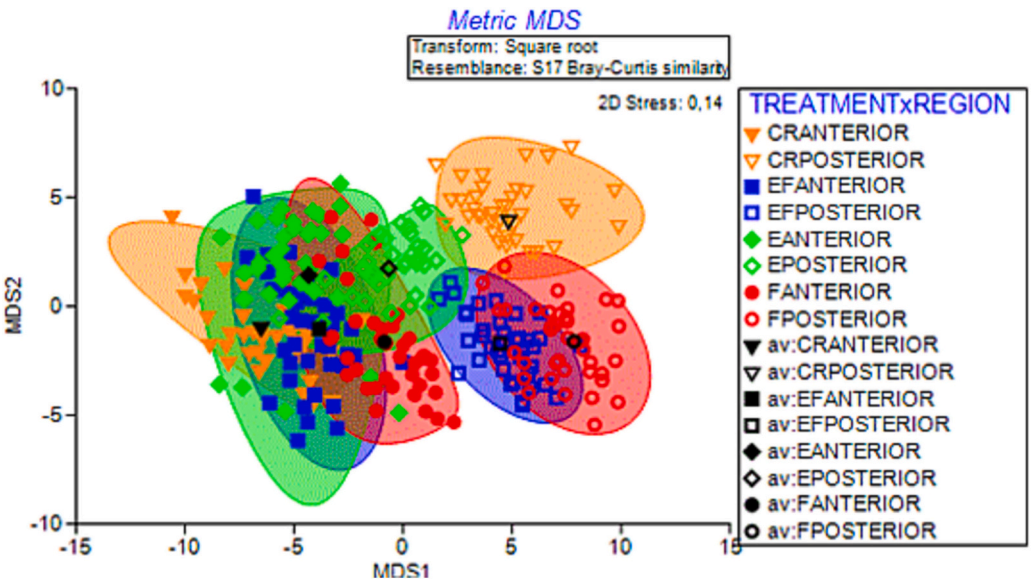

Fig. 7. MDS plot of group averages and confidence regions. The plot shows the effect of each diet (Treatment) on the expression of immune-related genes in each intestinal region (Anterior or Posterior). CT – Control diet; CR – diet with crude algae biomass; EF – diet with enzymatically hydrolysed and fermented algae biomass; E – diet with enzymatically hydrolysed algae biomass; F- diet with fermented algae biomass. The multivariate means plot was obtained from running the routine Bootstrap averages in PRIMER-e, which calculates and plots bootstrap averages and confidence regions by bootstrapping centroids of resemblance matrix groups. The centroids are calculated within a metric MDS of the resemblance matrix. MDS was selected to produce a final ordination plot including the confidence regions. PERMANOVA *P* values for pair-wise tests were: CRANTERIOR, CRPOSTERIOR =0.003; EFANTERIOR, EFPOSTERIOR = 0.004; FANTERIOR, FPOSTERIOR = 0.016; EANTERIOR, EPOSTERIOR = 0.357.

amino acid and peptide transporters and digestive enzymes located in the brush border membrane (BBM) of enterocytes. In examining the expression of amino acid solute carrier proteins, we did not aim for an exhaustive analysis. We focused on some members of the families SLC6 and SLC38, which are neutral amino acid transporters. The Slc6a18 and Slc6a19 are neutral amino acid transporters located at the apical membrane of intestinal and renal epithelia in mice (Bröer, 2014; Fairweather et al., 2015). In tilapia, they express in different segments of the intestine, and their expression is regulated by fasting and refeeding (Orozco et al., 2018). In the sea bass anterior intestine, incorporating *R. okamurae* in feeds did not affect the expression of *slc6a19b* and *slc6a18*. However, we detected significant downregulation of the *slc6a16a*. Little is known about Slc6a16 other than it is a sodium- and chloride-dependent neurotransmitter orphan transporter. Based on structure analysis, it is likely to function as a nutrient amino acid transporter (Castagna et al., 2022).

Members of the SLC38 family are Na^+ dependent neutral amino acid transporters, highly regulated by amino acid depletion (Bröer, 2014). In the sea bass intestine, feed manipulation did not affect the expression of the *slc38a3b*. Interestingly a solid significant downregulation was observed in the expression levels of the *slc38a2* in all groups except the F. This observation is relevant because this transporter is considered a transceptor (Hundal and Taylor, 2009), a plasma protein that may function not just as a transporter, but also have a separate function in signalling, with a potential regulatory role in the expression of other amino acid transporters. Further research on the function of Slc38a2 in regulating responses to feed composition and manipulation in aquaculture is guaranteed.

Several studies have reported that changes in diet composition can significantly modulate BBM enzyme activity in fish enterocytes (Krogdahl et al., 1999; Krogdahl and Bakke-McKellep, 2005; Tibaldi et al., 2006; Hamza et al., 2015; Tang et al., 2016). In the case of diets with plant-derived ingredients, the presence of anti-nutritional factors (ANFs), e.g., tannin, phytic acid, trypsin inhibitor, lectins, saponins, can hinder the bioavailability and digestibility of the nutrients and might cause improper amino acid balance (Francis et al., 2001). Our work in the sea bass did not find changes in the expression levels of the genes encoding the three BBM digestive enzymes (*anpep* for aminopeptidase N, AP-N; *alpi* for intestinal-type alkaline phosphatase, IAP; *si* for sucrase-isomaltase, SI) by the inclusion of *R. okamurae* biomass. AP-N and IAP are related to intestinal development and maturation (Imentai et al., 2022). AP-N plays a vital role in protein digestion, and IAP is involved in the absorption of nutrients such as lipids, glucose, calcium, and inorganic phosphate and is pivotal in controlling gut and systemic inflammation (Lallès, 2020). In turn, SI catalyses the hydrolysis of dietary carbohydrates, including starch, sucrose, and maltose, and a higher expression is usually an indicator of the species' flexibility toward an herbivorous profile (German et al., 2004). Previous studies have shown that protein levels and their source regulate AP-N gene expression levels in the grass carp (Tang et al., 2016). The expression of *alpi* increases in gilthead sea bream fed with processed animal proteins (Naya-Català et al., 2021) and by alterations in the gut microbiota composition in zebrafish (Bates et al., 2007). Expression levels of *si* increased in food-deprived European sea bass in a linear correlation with the expression levels of *anpep* (Hakim et al., 2009). In a recent study with *D. labrax* using a blend of two marine microalgae in a graded replacement (15% and 45%) of dietary fish meal (Messina et al., 2019), the authors reported no changes in the activity of the BBM enzymes maltase, sucrase-isomaltase, γ-glutamyl transferase and alkaline phosphatase. Nevertheless, they observed a significant increase in expression fold change, depending on the percentage of fish meal replacement, in *si* (1.5 and 1.9 respectively), *anpep* (1.87 and 1.99), and peptide transporter 1 (*slc15a1*; 1.4 and 1.5) in the anterior intestine of fish fed the microalgae-including diets. From their data set, the authors concluded that adding the blend of dried marine microalgae as an alternative to dietary fish meal did not hamper gut digestive-absorptive functions.

In our case, the lack of significant alterations in the expression of *anpep*, *alpi* and *si* suggests that the 5% algal biomass in the diets, irrespective of the pre-processing protocol, did not significantly change the expression signalling pattern of key digestive metabolism enzymes in the sea bass.

The gastrointestinal tract (GIT) plays the physiological role of digestion and absorption of nutrients but also ensures immune homeostasis by protecting from potentially harmful microorganisms while continuously being exposed to a load of dietary antigens and commensal bacteria (Ringø et al., 2010; Pichietti et al., 2021). One of the aspects that need assessment when using plant- or algae-derived diets to replace fish meal is the reaction of the immune system and the extent of

dysbiosis caused to the microbiota present in the GIT (Li et al., 2014; Ringø et al., 2016; Egerton et al., 2018; Limborg et al., 2018; Serra et al., 2021). Because gut microbiota composition is diet-dependent and influences host health and well-being, understanding how gut microbiota might shape gut immunity and modulate the immune response is paramount to evaluating and implementing alternative feed ingredients into aquafeeds.

To further characterize the impact of the four diets prepared with algae biomass, we analysed the composition of the intestinal fluid (digesta) microbiota through NGS, using composite samples, and the expression levels of immune-related genes in the anterior and posterior intestinal regions. A recent study characterized the sea bass gut microbiota using high-throughput sequencing in animals fed different diets, including plant-based diets (Serra et al., 2021). The overall composition of the bacterial community of *D. labrax* obtained in our work under the CT diet was comparable to the designated core microbiota found in those previous works. Proteobacteria and Bacteroidota essentially dominated, followed by Patescibacteria, Verrucomicrobiota and Actinobacteria with similar contributions, and finally by Firmicutes with a lower relative frequency. In our study, the CT diet already incorporates soymeal and wheat meal. Hence, a high relative frequency of Bacteroidota, considered a carbohydrate fermenting phylum (Pardesi et al., 2022), is to be expected. Interestingly, however, the relative frequency of Firmicutes, another carbohydrate fermenting phylum typical of herbivorous fish (Pardesi et al., 2022), shows a tendency to increase in the diets with algae biomass, except for F. However, the main impact of the algae-including diets is more evident in specific families within the Proteobacteria and Bacteroidota phyla, where an increase in the relative frequency of the family *Vibrionaceae* coincides with a marked decrease in *Flavobacteriaceae* and *Rhodobacteraceae*. That combined effect is more striking in the F diet. *Flavobacteriaceae* are primarily associated with nutrient acquisition, such as carbohydrate metabolism, and a recent study suggests the potential for diverse secondary metabolite biosynthesis (Gavriilidou et al., 2020). In turn, bacteria from *Rhodobacteraceae* positively correlate with growth performance (Huang et al., 2020), pathogen defence (Yao et al., 2018) and cold resistance (Liu et al., 2019) in shrimp.

In the present work, the decrease in the relative frequency of bacterial groups highlighted as playing a functional role in the digestion metabolism in the fish intestine is mostly evident in diets with pre-treated algae biomass. Apparently, the inclusion of the pre-digested algae biomass, albeit at 5%, was sufficient to cause different degrees of dysbiosis in what can be considered digestive core microbiota. However, we can rule out the impact of pre-treatment in the case of the CR diet. Instead, we suggest it is due to the inclusion of putative anti-nutrients of algal structural biomass, causing a substrate imbalance for the commensal bacteria. The bacterial community in the fish fed CR diet also showed the highest alfa diversity values, with an increase in the number of OTUs at low relative frequencies, suggesting an additional effect in the secondary microbiota elicited by the inclusion of the algae crude extract itself.

The marked increase in the relative frequency of *Vibrionaceae* was mainly due to an increase in *Vibrio* species. This observation prompted a closer inspection performed by running BLAST analyses in GenBank for each *Vibrio* sequence revealing the presence of OTUs ascribed to the clades Harvey, Anguillarum, Splendidus and Mediterranean (data not shown). All these clades harbour provable or putative pathogenic *Vibrio* species for marine animals. Since we did not analyse the mucosa microbiota, we cannot extrapolate if these high relative frequencies were limited to merely opportunistic *Vibrio* in the digesta or if an underlying pathogenic situation was developing. Nevertheless, the high relative frequency of *Vibrio* in the digesta did not significantly affect K index. However, it might have created an immune challenge, ultimately contributing indirectly to the reduced final body mass observed in the CR, E and F groups.

In the present work, we quantified the expression level of three types of cytokines (interferon-gamma, two chemokines, and six interleukins) in the anterior and posterior intestines. No significant effect was observed in the E group in both intestinal segments, despite the high relative frequency of *Vibrionaceae* in the microbiota. Of the nine genes under analysis, the expression of *il6* was significantly altered only in the anterior intestine and only in the fish fed EF diet. This interleukin is considered a key pro-inflammatory, inducible by lipopolysaccharides (LPS), the endotoxin of Gram-negative bacteria. It promotes the proliferation of macrophages and B cells and up-regulates antimicrobial peptide (AMP) gene expression in macrophages (Zou and Secombes, 2016). In contrast to the anterior intestine, more genes had their expression altered in the posterior intestine. This observation is consistent with evidence gathered by other authors, with different fish species, establishing the posterior intestine as the intestinal region more reactive for most of the immune-related genes studied (Pichietti et al., 2021, and references therein).

In the posterior intestine, animals fed the EF and F diets showed a significant increase in the expression level of *ifng* and *il10*. IFN-γ and IL-10 are associated with type M1 and type M2 macrophages, respectively (Muraille et al., 2014). Th1 cells mediate the conversion of M1 into a potent antimicrobial effector cell that activates infected macrophages through cell contact and the focal secretion of IFN-γ. Th2 cells, in turn, are involved in the induction of the alternatively activated macrophage phenotype (M2), which mediates resolution of the inflammatory stage and initiates tissue repair in wound healing processes and maintains tissue integrity (Muraille et al., 2014).

It was previously suggested that the IL-10-mediated immune responses involve the fine-tuned regulation of cytokines, including IFN-γ and IL-10 itself, by enhancing the expression of suppressors of cytokine signalling (SOCS) proteins (Ding et al., 2003). The effect of fish IFN-γ on the activation of M1 macrophage is the induction of the typical immune profile: inflammation, increased respiratory burst and nitric oxide production (Pereiro et al., 2019) to establish the first line of defence against intracellular pathogens. M2 macrophages, on the other hand, play a predominant role in the suppression of immune responses (Martinez et al., 2008) and are known in teleosts to express immunosuppressive cytokines such as IL-10 (Grayfer et al., 2011; Castro et al., 2011). IL-10 is considered a cytokine with a vital role in the termination of inflammatory responses, development of long-lived memory cells and successful restoration of homeostasis (Piazzon et al., 2015). In fact, experiments with carp macrophage cell culture revealed an anti-inflammatory role for IL-10 (Piazzon et al., 2015), which involved increased expression of *ifng* and *il10* and decreased *il12* transcripts in neutrophils stimulated with LPS. In turn, in zebrafish, an IL-10–mediated suppression of Th1 cell response and cytokine production was reported with *Mycobacterium marinum* infection (Harjula et al., 2018). Also in zebrafish, with gut inflammation caused by food antigens, an increase in *il10* transcripts was previously interpreted as a polarization of T cells toward a tolerogenic profile and functional adaptive immune response (Coronado et al., 2019).

In contrast to the response to the EF and F diets, significant increases in *il8* and *il12b* expression levels were present in the posterior intestine of animals fed the CR diet, while although a slight increase in *infg* and *il10* transcripts could be observed, it was not significant. A putative role in the launch of the immune response in teleosts has been suggested for IL-8 and IL-12. Expression levels of *il8* were found to correlate with early stages of the inflammatory process in the intestine of zebrafish larvae upon change to a soymeal-including diet (Coronado et al., 2019). Also, transcripts for both these pro-inflammatory interleukins are known to be increased by LPS in carp (Piazzon et al., 2015; Arts et al., 2010), and downregulated by IL-10 (Piazzon et al., 2015).

In our work, and considering the literature evidence, we suggest that in the case of the EF and F diet, *D. labrax* was able to develop an adaptive immune response to the combined effect of algae biomass inclusion and proliferation of potential pathogenic microbiota. In turn, the exclusively pro-inflammatory response observed in the CR group could indicate a

weaker inflammatory process, a delayed development of the immune response or even a lack of capacity to overcome the intolerance to putative ANFs in the algae biomass.

5. Conclusions

In conclusion, we believe that 5% dietary inclusion of *R. okamurae* biomass could be a suitable raw material for aquafeeds in the European sea bass. Other species will obviously need testing. However, using *R. okamurae* biomass requires a pre-treatment before inclusion, preferably involving enzymatic hydrolysis and fermentation. Otherwise, while the fish still have a positive growth performance, the gastrointestinal tract pays a toll on the integrity, transport, and inflammatory processes. This work showed that it is possible to produce pre-treated algal biomass to obtain adequate growth performance in this fish species. Nevertheless, dietary inclusion of treated *R. okamurae* still requires further studies to fully characterize its suitability.

CRediT authorship contribution statement

Filomena Fonseca: Investigation, Formal analysis, Data curation, Visualization, Writing – original draft, Writing – review & editing. **Juan Fuentes:** Conceptualization, Methodology, Investigation, Writing – review & editing. **Antonio Jesús Vizcaíno:** Resources, Funding acquisition. **Francisco Javier Alarcón:** Resources, Funding acquisition. **Juan Miguel Mancera:** Resources, Funding acquisition. **Gonzalo Martínez-Rodríguez:** Methodology, Data curation, Writing – review & editing. **Juan Antonio Martos-Sitcha:** Investigation, Resources, Funding acquisition, Writing – review & editing.

Declaration of Competing Interest

The authors declare that there is no conflict of interest regarding the publication of this article.

Data availability

Data will be made available on request.

Acknowledgements

The authors wish to thank Felix López Figueroa, Juan José Quintero Díaz and Candela Sánchez Atienza for their help in collecting the seaweed biomass with the permission of *Delegación Territorial de Agricultura, Ganadería, Pesca y Desarrollo Sostenible* in Cádiz. This research was supported by the Projects VALINVA (*Proyecto de Innovación Empresarial con Proyección Territorial en el Ámbito de la Economía Azul* CEI·MAR*CEIMAR 2019*) and Bluemaro (PID2020-116136RB-I00, Ministerio de Ciencia e Innovación, Spain) granted to JAM-S and FJA, respectively, and the Spin-off LifeBioencapsulation S.L.

We also acknowledge the support of the University of Almería (Experimental feeds Service, https://www.ual.es/universidad/servicios generales/stecnicos/perifericos-convenio/piensos-experimentales) on aquafeed elaboration. Experimental feeds Service was granted by EQC2018-004984-P and EQC2019-006380-P.

CCMar receives Portuguese national funds from FCT - Foundation for Science and Technology through projects UIDB/04326/2020, UIDP/04326/2020 and LA/P/0101/2020.

CIMA receives Portuguese national funds from FCT - Foundation for Science and Technology through project UIDP/00350/2020.

ARNET, Associate Laboratory, receives Portuguese national funds from FCT - Foundation for Science and Technology through project LA/P/0069/2020.

Filomena Fonseca was supported by a grant from Fundación Carolina during her sabbatical stay at UCA and ICMAN.

Appendix A. Supplementary data

Supplementary data to this article can be found online at https://doi.org/10.1016/j.aquaculture.2023.739318.

References

Alves, A., Gregório, S.F., Egger, R.C., Fuentes, J., 2019. Molecular and functional regionalization of bicarbonate secretion cascade in the intestine of the European sea bass (*Dicentrarchus labrax*). Comp. Biochem. Physiol. Part - C: Toxicol. Pharmacol. 233, 53–64. https://doi.org/10.1016/j.cbpa.2019.03.017.

Andrews, S., 2010. FastQC: A quality control tool for high throughput sequence data. https://www.bioinformatics.babraham.ac.uk/projects/fastqc/.

AOAC, 2000. Official Methods of Analysis, 17th edition. Association of Official Analytical Chemists, Washington DC.

Arnold, Y.E., Thorens, J., Bernard, S., Kalia, Y.N., 2019. Drug transport across porcine intestine using an Ussing chamber system: regional differences and the effect of P-glycoprotein and CYP3A4 activity on drug absorption. Pharmaceutics 11, 139. https://doi.org/10.3390/pharmaceutics11030139.

Arts, J.A.J., Tijhaar, E.J., Chadzinska, M., Savelkoul, H.F.J., Verburg-van Kemenade, B. M.L., 2010. Functional analysis of carp interferon-Υ: evolutionary conservation of classical phagocyte activation. Fish Shellfish Immunol. 29, 793–802. https://doi.org/10.1016/j.fsi.2010.07.010.

Balda, M.S., Whitney, J.A., Flores, C., González, S., Cereijido, M., Matter, K., 1996. Functional dissociation of paracellular permeability and transepithelial electrical resistance and disruption of the apical-basolateral intramembrane diffusion barrier by expression of a mutant tight junction membrane protein. J. Cell Biol. 134, 1031–1049. https://doi.org/10.1083/jcb.134.4.1031.

Bates, J.M., Akerlund, J., Mittge, E., Guillemin, K., 2007. Intestinal alkaline phosphatase detoxifies lipopolysaccharide and prevents inflammation in zebrafish in response to gut microbiota. Cell Host Microbe 2, 371–382. https://doi.org/10.1016/j.chom.2007.10.010.

Batista, S., Pereira, R., Oliveira, B., Baião, L.F., Jessen, F., Tulli, F., Messina, M., Silva, J. L., Abreu, H., Valente, L.M.P., 2020. Exploring the potential of seaweed *Gracilaria gracilis* and microalga *Nannochloropsis oceanica*, single or blended, as natural dietary ingredients for European seabass *Dicentrarchus labrax*. J. Appl. Phycol. 32, 2041–2059. https://doi.org/10.1007/s10811-020-02118-z.

Bröer, S., 2014. The SLC38 family of sodium-amino acid co-transporters. Pflugers Arch. 466, 155–172. https://doi.org/10.1007/s00424-013-1393-y.

Callahan, B.J., McMurdie, P.J., Rosen, M.J., Han, A.W., Johnson, A.J.A., Holmes, S.P., 2016. DADA2: high-resolution sample inference from Illumina amplicon data. Nat. Methods 13, 581–583. https://doi.org/10.1038/nmeth.3869.

Caporaso, J., Kuczynski, J., Stombaugh, J., Bittinger, K., Bushman, F.D., Costello, E.K., Fierer, N., Peña, A.G., Goodrich, J.K., Gordon, J.I., Huttley, G.A., Kelley, S.T., Knights, D., Koenig, J.E., Ley, R.E., Lozupone, C.A., McDonald, D., Muegge, B.D., Pirrung, M., Reeder, J., Sevinsky, J.R., Turnbaugh, P.J., Walters, W.A., Widmann, J., Yatsunenko, T., Zaneveld, J., Knight, R., 2010. QIIME allows analysis of high-throughput community sequencing data. Nat. Methods 7, 335–336. https://doi.org/10.1038/nmeth.f.303.

Casal-Porras, I., Zubía, E., Brun, F.G., 2021. Dilkamural: a novel chemical weapon involved in the invasive capacity of the alga *Rugulopteryx okamurae* in the Strait of Gibraltar. Estuar. Coast. Shelf S. 257, 107398 https://doi.org/10.1016/j.ecss.2021.107398.

Castagna, M., Cinquetti, R., Verri, T., Vacca, F., Giovanola, M., Barca, A., Romanazzi, T., Roseti, C., Galli, A., Bossi, E., 2022. The lepidopteran KAAT1 and CAATCH1: orthologs to understand structure-function relationships in mammalian SLC6 transporters. Neurochem. Res. 47, 111–126. https://doi.org/10.1007/s11064-021-03410-1.

Castro, R., Zou, J., Secombes, C.J., Martin, S.A.M., 2011. Cortisol modulates the induction of inflammatory gene expression in a rainbow trout macrophage cell line. Fish Shellfish Immunol. 30, 215–223. https://doi.org/10.1016/j.fsi.2010.10.010.

Clarke, K.R., Gorley, R.N., Somerfield, P.J., Warwick, R.M., 2014. Change in Marine Communities: An Approach to Statistical Analysis and Interpretation, 3rd edition. PRIMER-E, Plymouth. https://updates.primer-e.com/primer7/manuals/Methods_manual_v7.pdf.

Coronado, M., Solis, C.J., Hernandez, P.P., Feijoó, C.G., 2019. Soybean meal-induced intestinal inflammation in zebrafish is T cell-dependent and has a Th17 cytokine profile. Front. Immunol. 10, 610. https://doi.org/10.3389/fimmu.2019.00610.

Demuez, M., Mahdy, A., Tomás-Pejó, E., González-Fernández, C., Ballesteros, M., 2015. Enzymatic cell disruption of microalgae biomass in biorefinery processes. Biotechnol. Bioeng. 112, 1955–1966. https://doi.org/10.1002/bit.25644.

Ding, Y., Chen, D., Tarcsafalvi, A., Su, R., Qin, L., Bromberg, J.S., 2003. Suppressor of cytokine signalling 1 inhibits IL-10-mediated immune responses. J. Immunol. 170, 1383–1391. https://doi.org/10.4049/jimmunol.170.3.1383.

Egerton, S., Culloty, S., Whooley, J., Stanton, C., Ross, R.P., 2018. The gut microbiota of marine fish. Front. Microbiol. 9, 873. https://doi.org/10.3389/fmicb.2018.00873.

El-tawil, N.E., 2010. Effects of green seaweeds (*Ulva* sp.) as feed supplements in red Tilapia (*Oreochromis* sp.) diet on growth performance, feed utilization and body composition. J. Arabian Aquacult. Soc. 5, 179–193. http://arabaqs.org/journal/vol_5/2/Text%2010%20-%2013.pdf.

Estensoro, I., Ballester-Lozano, G., Benedito-Palos, L., Grammes, F., Martos-Sitcha, J.A., Mydland, L.-T., Calduch-Giner, J.A., Fuentes, J., Karalazos, V., Ortiz, A., Øverland, M., Sitjá-Bobadilla, A., Pérez-Sánchez, P., 2016. Dietary butyrate helps to restore the intestinal status of a marine teleost (*Sparus aurata*) fed extreme diets low

in fish meal and fish oil. PLoS One 11, e0166564. https://doi.org/10.1371/journal.pone.0166564.
Fairweather, S.J., Bröer, A., Subramanian, N., Tumer, E., Cheng, Q., Schmoll, D., O'Mara, M.L., Bröer, S., 2015. Molecular basis for the interactions of the mammalian amino acid transporters B(0)AT1 and B(0)AT3 with their ancillary protein collectrin. J. Biol. Chem. 290, 24308–24325. https://doi.org/10.1074/jbc.M115.648519.
Felix, N., Brindo, R.A., 2014. Evaluation of raw and fermented seaweed, *Ulva lactuca* as feed ingredient in giant freshwater prawn *Macrobrachium rosenbergii*. Int. J. Fish Aquat. Stud. 1 (3), 199–204. https://www.fisheriesjournal.com/archives/2014/vol1issue3/PartC/15.pdf.
Fernandes, H., Martins, N., Vieira, L., Salgado, J.M., Castro, C., Oliva-Teles, A., Belo, I., Peres, H., 2022. Pre-treatment of *Ulva rigida* improves its nutritional value for European seabass (*Dicentrarchus labrax*) juveniles. Algal Res. 66, 102803 https://doi.org/10.1016/j.algal.2022.102803.
Folch, J., Lees, M., Sloane Stanley, G.H., 1957. A simple method for the isolation and purification of total lipids from animal tissues. J. Biol. Chem. 226 (1), 497–509. https://doi.org/10.1016/S0021-9258(18)64849-5.
Francis, G., Makkar, H.P.S., Becker, K., 2001. Antinutritional factors present in plant-derived alternate fish feed ingredients and their effects in fish. Aquaculture 199, 197–227. https://doi.org/10.1016/S0044-8486(01)00526-9.
Fuentes, J., Power, D.M., Canario, A.V., 2010. Parathyroid hormone-related protein-stanniocalcin antagonism in regulation of bicarbonate secretion and calcium precipitation in a marine fish intestine. Am. J. Phys. Regul. Integr. Comp. Phys. 299, R150–R158. https://doi.org/10.1152/ajpregu.00378.2009.
García-Gómez, J.C., Sempere-Valverde, J., González, A.R., Martínez-Chacón, M., Olaya-Ponzone, L., Sánchez-Moyano, E., Megina, C., 2020. From exotic to invasive in record time: the extreme impact of *Rugulopteryx okamurae* (Dictyotales, Ochrophyta) in the strait of Gibraltar. Sci. Total Environ. 704, 135408 https://doi.org/10.1016/j.scitotenv.2019.135408.
Gavriilidou, A., Gutleben, J., Versluis, D., Forgiarini, F., van Passel, M.W.J., Ingham, C.J., Smidt, H., Sipkema, D., 2020. Comparative genomic analysis of *Flavobacteriaceae*: insights into carbohydrate metabolism, gliding motility and secondary metabolite biosynthesis. BMC Genomics 21, 569. https://doi.org/10.1186/s12864-020-06971-7.
German, D.P., Horn, M.H., Gawlicka, A., 2004. Digestive enzyme activities in herbivorous and carnivorous prickleback fishes (Teleostei: Stichaeidae): ontogenetic, dietary, and phylogenetic effects. Physiol. Biochem. Zool. 77, 789–804. https://doi.org/10.1086/422228.
Grayfer, L., Hodgkinson, J.W., Hitchen, S.J., Belosevic, M., 2011. Characterization and functional analysis of goldfish (*Carassius auratus* L.) interleukin-10. Mol. Immunol. 48, 563–571. https://doi.org/10.1016/j.molimm.2010.10.013.
Hakim, Y., Harpaz, S., Uni, Z., 2009. Expression of brush border enzymes and transporters in the intestine of European sea bass (*Dicentrarchus labrax*) following food deprivation. Aquaculture 290, 110–115. https://doi.org/10.1016/j.aquaculture.2009.02.008.
Hamza, N., Ostaszewska, T., Kestemont, P., 2015. Development and functionality of the digestive system in percid fishes early life stages. In: Kestemont, P., Dabrowski, K., Summerfelt, R. (Eds.), Biology and Culture of Percid Fishes. Springer, Dordrecht, pp. 239–264. https://doi.org/10.1007/978-94-017-7227-3_8.
Harjula, S.-K.E., Ojanen, M.J.T., Taavitsainen, S., Nykter, M., Rämet, M., 2018. Interleukin 10 mutant zebrafish have an enhanced interferon gamma response and improved survival against a *Mycobacterium marinum* infection. Sci. Rep. 8, 10360. https://doi.org/10.1038/s41598-018-28511-w.
Huang, L., Guo, H., Chen, C., Huang, X., Chen, W., Bao, F., Liu, W., Wang, S., Zhang, D., 2020. The bacteria from large-sized bioflocs are more associated with the shrimp gut microbiota in culture system. Aquaculture 523, 735159. https://doi.org/10.1016/j.aquaculture.2020.735159.
Hundal, H.S., Taylor, P.M., 2009. Amino acid transceptors: gate keepers of nutrient exchange and regulators of nutrient signalling. Am. J. Physiol. Endocrinol. Metab. 296, E603–E613. https://doi.org/10.1152/ajpendo.91002.2008.
Imentai, A., Gilannejad, N., Martínez-Rodríguez, G., López, F.J., Martínez, F.P., Peňka, T., Dzyuba, V., Dadras, H., Policar, T., 2022. Effects of first feeding regime on gene expression and enzyme activity in pikeperch (*Sander lucioperca*) larvae. Front. Mar. Sci. 9, 864536 https://doi.org/10.3389/fmars.2022.864536.
Klindworth, A., Pruesse, E., Schweer, T., Peplies, J., Quast, C., Horn, M., Glöckner, F.O., 2013. Evaluation of general 16S ribosomal RNA gene PCR primers for classical and next-generation sequencing-based diversity studies. Nucleic Acids Res. 41 (1), e1 https://doi.org/10.1093/nar/gks808.
Koressaar, T., Remm, M., 2007. Enhancements and modifications of primer design program Primer3. Bioinformatics 23, 1289–1291. https://doi.org/10.1093/bioinformatics/btm091.
Krogdahl, A., Bakke-McKellep, A.M., 2005. Fasting and refeeding cause rapid changes in intestinal tissue mass and digestive enzyme capacities of Atlantic salmon (*Salmo salar* L.). Comp. Biochem. Phys. A Mol. Integr. Physiol. 141A, 450–460. https://doi.org/10.1016/j.cbpb.2005.06.002.
Krogdahl, A., Nordrum, S., Sørensen, M., Brudeseth, L., Røsjø, C., 1999. Effects of diet composition on apparent nutrient absorption along the intestinal tract and of subsequent fasting on mucosal disaccharidase activities and plasma nutrient concentration in Atlantic salmon *Salmo salar* L. Aquac. Nutr. 5, 121–133. https://doi.org/10.1046/j.1365-2095.1999.00095.x.
Lallès, J.P., 2020. Intestinal alkaline phosphatase in the gastrointestinal tract of fish: biology, ontogeny, and environmental and nutritional modulation. Rev. Aquac. 555–581 https://doi.org/10.1111/raq.12340.
Li, J., Ni, J., Li, J., Wang, C., Li, X., Wu, S., Zhang, T., Yu, Y., Yan, Q., 2014. Comparative study on gastrointestinal microbiota of eight fish species with different feeding habits. J. Appl. Microbiol. 117, 1750–1760. https://doi.org/10.1111/jam.12663.
Limborg, M.T., Alberdi, A., Kodama, M., Roggenbuck, M., Kristiansen, K., Gilbert, M.T.P., 2018. Applied hologenomics: feasibility and potential in aquaculture. Trends Biotechnol. 36, 252–264. https://doi.org/10.1016/j.tibtech.2017.12.006.
Liu, J., Wang, K., Wang, Y., Chen, W., Jin, Z., Yao, Z., Zhang, D., 2019. Strain-specific changes in the gut microbiota profiles of the white shrimp *Litopenaeus vannamei* in response to cold stress. Aquaculture 503, 357–366. https://doi.org/10.1016/j.aquaculture.2019.01.026.
Martinez, F.O., Sica, A., Mantovani, A., Locati, M., 2008. Macrophage activation and polarization. Front. Biosci. 13, 453–461. https://doi.org/10.2741/2692.
Martínez-Antequera, F.P., Martos-Sitcha, J.A., Reyna, J.M., Moyano, F.J., 2021. Evaluation of the inclusion of the green seaweed *Ulva ohnoi* as an ingredient in feeds for gilthead seabream (*Sparus aurata*) and European seabass (*Dicentrarchus labrax*). Animals. 11, 1684. https://doi.org/10.3390/ani11061684.
Messina, M., Bulfon, G., Beraldo, P., Tibaldi, E., Cardinaletti, G., 2019. Intestinal morpho-physiology and innate immune status of European seabass (*Dicentrarchus labrax*) in response to diets including a blend of two marine microalgae, *Tisochrysis lutea* and *Tetraselmis suecica*. Aquaculture 500, 660–669. https://doi.org/10.1016/j.aquaculture.2018.09.054.
Miglavs, I., Jobling, M., 1989. The effect of feeding regime on proximate body composition and patterns of energy deposition in juvenile Arctic charr, *Salvelinus alpinus*. J. Fish Biol. 35, 1–11. https://doi.org/10.1111/j.1095-8649.1989.tb03387.x.
Molina-Roque, L., Bárany, A., Sáez, M.I., Alarcón, F.J., Tapia, S.T., Fuentes, J., Mancera, J.M., Perera, E., Martos-Sitcha, J.A., 2022. Biotechnological treatment of microalgae enhances growth performance, hepatic carbohydrate metabolism and intestinal physiology in gilthead seabream (*Sparus aurata*) juveniles close to commercial size. Aquacult. Rep. 25, 101248 https://doi.org/10.1016/j.aqrep.2022.101248.
Moutinho, S., Linares, F., Rodríguez, J.L., Sousa, V., Valente, L.M.P., 2018. Inclusion of 10% seaweed meal in diets for juvenile and on-growing life stages of Senegalese sole (*Solea senegalensis*). J. Appl. Phycol. https://doi.org/10.1007/s10811-018-1482-6.
Muraille, E., Oberdan, L., Moser, M., 2014. Th1/Th2 paradigm extended: macrophage polarization as an unappreciated pathogen-driven escape mechanism? Front. Immunol. 5, 603. https://doi.org/10.3389/fimmu.2014.00603.
Naya-Català, F., do Vale Pereira, G., Piazzon, M.C., Fernandes, A.M., Calduch-Giner, J.A., Sitjà-Bobadilla, A., Conceição, L.E.C., Pérez-Sánchez, J., 2021. Cross-talk between intestinal microbiota and host gene expression in gilthead sea bream (*Sparus aurata*) juveniles: insights in fish feeds for increased circularity and resource utilization. Front. Physiol. 12, 748265 https://doi.org/10.3389/fphys.2021.748265.
Orozco, Z.G.A., Soma, S., Kaneko, T., Watanabe, S., 2018. Spatial mRNA expression and response to fasting and refeeding of neutral amino acid transporters slc6a18 and slc6a19a in the intestinal epithelium of Mozambique tilapia. Front. Physiol. 13, 212. https://doi.org/10.3389/fphys.2018.00212.
Pardesi, B., Roberton, A.M., Lee, K.C., Angert, E.R., Rosendale, D.I., Boycheva, S., White, W.L., Clements, K.D., 2022. Distinct microbiota composition and fermentation products indicate functional compartmentalization in the hindgut of a marine herbivorous fish. Mol. Ecol. 00, 1–16. https://doi.org/10.1111/mec.16394.
Paula, J.C.D., Vallim, M.A., Teixeira, V.L., 2011. What are and where are the bioactive terpenoids metabolites from Dictyotaceae (Phaeophyceae). Rev. Bras 21, 216–228. https://doi.org/10.1590/S0102-695X2011005000079.
Peixoto, M.J., Salas-Leitón, E., Ferreira Pereira, L., Queiroz, A., Magalhães, F., Pereira, R., Abreu, H., Reis, P.A., Magalhães Gonçalves, J.F., Ozório, R.O.A., 2016. Role of dietary seaweed supplementation on growth performance, digestive capacity and immune and stress responsiveness in European seabass (*Dicentrarchus labrax*). Aquacult. Rep. 3, 189–197. https://doi.org/10.1016/j.aqrep.2016.03.005.
Peixoto, M.J., Ferraz, R., Magnoni, L.J., Pereira, R., Gonçalves, J.F., Calduch-Giner, J., Pérez-Sánchez, J., Ozório, R.O.A., 2019. Protective effects of seaweed supplemented diet on antioxidant and immune responses in European seabass (*Dicentrarchus labrax*) subjected to bacterial infection. Sci. Rep. 9, 16134. https://doi.org/10.1038/s41598-019-52693-6.
Pereiro, P., Figueras, A., Novoa, B., 2019. Insights into teleost interferon-gamma biology: an update. Fish Shellfish Immun. 90, 150–164. https://doi.org/10.1016/j.fsi.2019.04.002.
Pfaffl, M.W., 2001. A new mathematical model for relative quantification in real-time RT-PCR. Nucleic Acids Res. 29 (9), e45 https://doi.org/10.1093/nar/29.9.e45.
Piazzon, M.C., Savelkoul, H.S.J., Pietretti, D., Wiegertjes, G.F., Forlenza, M., 2015. Carp Il10 has anti-inflammatory activities on phagocytes, promotes proliferation of memory T cells, and regulates B cell differentiation and antibody secretion. J. Immunol. 194, 187–199. https://doi.org/10.4049/jimmunol.1402093.
Pichietti, S., Miccoli, A., Fausto, A.M., 2021. Gut immunity in European sea bass (*Dicentrarchus labrax*): a review. Fish Shellfish Immun. 108, 94–108. https://doi.org/10.1016/j.fsi.2020.12.001.
Reis, B., Ramos-Pinto, L., Martos-Sitcha, J.A., Machado, M., Azeredo, R., Fernández-Boo, S., Engrola, S., Unamunzaga, C., Calduch-Giner, J., Conceição, L.E.C., Silva, T., Dias, J., Costas, B., Pérez-Sánchez, J., 2021. Health status in gilthead seabream (*Sparus aurata*) juveniles fed diets devoid of fishmeal and supplemented with *Phaeodactylum tricornutum*. J. Appl. Phycol. 33, 979–996. https://doi.org/10.1007/s10811-021-02377-4.
Ringø, E., Løvmo, L., Kristiansen, M., Bakken, Y., Salinas, I., Myklebust, R., Olsen, R.E., Mayhew, T.M., 2010. Lactic acid bacteria vs. pathogens in the gastrointestinal tract of fish: a review. Aquac. Res. 41, 451–467. https://doi.org/10.1111/j.1365-2109.2009.02339.x.
Ringø, E., Zhou, Z., Vecino, J.L.G., Wadsworth, S., Romero, J., Krogdahl, Å., Olsen, R.E., Dimitroglou, A., Foey, A., Davies, S., Owen, M., Lauzon, H.L., Martinsen, L.L., De Schyver, P., Bossier, P., Perstad, S., Merrifield, D.L., 2016. Effect of dietary

components on the gut microbiota of aquatic animals. A never-ending story? Aquac. Nutr. 22, 219–282. https://doi.org/10.1111/anu.12346.
Sáez, M.I., Galafat, A., Vizcaíno, A.J., Chaves-Pozo, E., Ayala, M.D., Arizcun, M., Alarcón, F.J., Suárez, M.D., Martínez, T.F., 2022. Evaluation of *Nannochloropsis gaditana* raw and hydrolysed biomass at low inclusion level as dietary functional additive for gilthead seabream (*Sparus aurata*) juveniles. Aquaculture 556, 738288. https://doi.org/10.1016/j.aquaculture.2022.738288.
Serra, C.R., Oliva-Teles, A., Enes, P., Tavares, F., 2021. Gut microbiota dynamics in carnivorous European seabass (*Dicentrarchus labrax*) fed plant-based diets. Sci. Rep. 11, 447. https://doi.org/10.1038/s41598-020-80138-y.
Silva, D.M., Valente, L.M.P., Sousa-Pinto, I., Pereira, R., Pires, M.A., Seixas, F., Rema, P., 2015. Evaluation of IMTA-produced seaweeds (*Gracilaria*, *Porphyra*, and *Ulva*) as dietary ingredients in Nile tilapia, *Oreochromis niloticus* L., juveniles. Effects on growth performance and gut histology. J. Appl. Phycol. 27, 1671–1680. https://doi.org/10.1007/s10811-014-0453-9.
Siriwardhana, N., Jeon, Y.-J., Kim, S.-H., Há, J.-H., Heo, S.-J., Lee, K.-W., 2004. Enzymatic hydrolysis for effective extraction of antioxidative compounds from *Hizikia fusiformis*. Algae 19, 59–68. https://doi.org/10.4490/ALGAE.2004.19.1.059.
Steen, F., Aragay, J., Zuljevic, A., Verbruggen, H., Mancuso, F.P., Bunker, F., Vitales, D., Gómez Garreta, A., De Clerck, O., 2017. Tracing the introduction history of the brown seaweed *Dictyota cyanoloma* (Phaeophyceae, Dictyotales) in Europe. Eur. J. Phycol. 52, 31–42. https://doi.org/10.1080/09670262.2016.1212998.
Tang, J., Qu, F., Tang, X., Zhao, Q., Wang, Y., Zhou, Y., Feng, J., Lu, S., Hou, D., Liu, Z., 2016. Molecular characterization and dietary regulation of aminopeptidase N (APN) in the grass carp (*Ctenopharyngodon idella*). Gene 582, 77–84. https://doi.org/10.1016/j.gene.2016.01.046.
Tibaldi, E., Hakim, Y., Uni, Z., Tulli, F., de Francesco, M., Luzzana, U., Harpaz, S., 2006. Effects of the partial substitution of dietary fish meal by differently processed soybean meals on growth performance, nutrient digestibility and activity of intestinal brush border enzymes in the European sea bass (*Dicentrarchus labrax*). Aquaculture 261, 182–193. https://doi.org/10.1016/j.aquaculture.2006.06.026.
Tibbetts, S.M., 2018. The potential for 'next-generation', microalgae-based feed ingredients for salmonid aquaculture in context of the blue revolution. In: Jacob-Lopes, E., Zepka, L.Q., Queiroz, M.I. (Eds.), Microalgal Biotechnology. IntechOpen, London. https://doi.org/10.5772/intechopen.73551.
Untergasser, A., Cucutache, I., Koressaar, T., Ye, J., Faircloth, B.C., Remm, M., Rozen, S. G., 2012. Primer3 – new capabilities and interfaces. Nucleic Acids Res. 40, e115 https://doi.org/10.1093/nar/gks596.
Valente, L.M.P., Gouveia, A., Rema, P., Matos, J., Gomes, E.F., Pinto, I.S., 2006. Evaluation of three seaweeds *Gracilaria bursa-pastoris*, *Ulva rigida* and *Gracilaria cornea* as dietary ingredients in European sea bass (*Dicentrarchus labrax*) juveniles. Aquaculture 252, 85–91. https://doi.org/10.1016/j.aquaculture.2005.11.052.
Van Itallie, C.M., Anderson, J.M., 2014. Architecture of tight junctions and principles of molecular composition. Semin. Cell Dev. Biol. 36, 157–165. https://doi.org/10.1016/j.semcdb.2014.08.011.
Yao, Z., Yang, K., Huang, L., Huang, X., Qiuqian, L., Wang, K., Zhang, D., 2018. Disease outbreak accompanies the dispersive structure of shrimp gut bacterial community with a simple core microbiota. AMB Express 8, 1–10. https://doi.org/10.1186/s13568-018-0644-x.
Zhu, D., Wen, X., Xuan, X., Li, S., Li, Y., 2016. The green alga *Ulva lactuca* as a potential ingredient in diets for juvenile white spotted snapper *Lutjanus stellatus* Akazaki. J. Appl. Phycol. 28, 703–711. https://doi.org/10.1007/s10811-015-0545-1.
Zou, J., Secombes, C.J., 2016. The function of fish Cytokines. Biology 5, 23. https://doi.org/10.3390/biology5020023.